Supporting Information

Development of a concise and robust route to a key fragment of MCL-1 inhibitors via stereoselective defluoroborylation

Matthieu Jouffroy[a]*, Philip Pye[b], Soufyan Jerhaoui[c], Wenyong Chen[d], Michel Surkyn[c]

[a] *Chemical Process R&D, Discovery Process Research, Janssen Pharmaceutica N.V, Turnhoutseweg 30, 2340 Beerse, Belgium*

[b] *Chemical Process R&D, External Research and Development Capabilities, Janssen Research & Development LLC, 920 US Route 202, PO Box 300, New Jersey 08869, United States*

[c] *Discovery Science, Discovery Chemistry BE, Janssen Pharmaceutica N.V, Turnhoutseweg 30, 2340 Beerse, Belgium;*

[d] *Chemical Process R&D, Discovery Process Research, Janssen Research & Development LLC, Spring House, Pennsylvania 19477, USA*

*Email: mjouffro@its.jnj.com

Contents

I. General information on High Throughput Experimentation (HTE)

Unless otherwise noted, all reactions were performed in an Innovative glovebox operating on its catalyst bed with oxygen levels typically < 5 ppm. Reaction experimental design was aided by the use of Unchained® Library Studio. Reactions run at 10 µmol scale for the limiting reagent were carried out in 1 mL glass vials (Analytical-Sales) equipped with magnetic tumble stir bars (V&P Scientific) in 24 or 96-well reactor blocks (Analytical-Sales). The various compounds were handled as liquids using single and multi-channel pipettors (Eppendorf, 10, 100, 200, and 1000 µL). On completion of solution dosing the plates were covered by a perfluoroalkoxy alkane (PFA) mat (Analytical-Sales), followed by two silicon rubber mats (Analytical-Sales), and an aluminum cover which was tightly and evenly sealed by 9 screws. The plate was removed from the glovebox and placed in a heating block (V&P Scientific) on the top a magnetic tumble stirrer (500 rpm) and heated to the appropriate temperature. After 16 h, the plate was unsealed and reaction mixtures were diluted with a quench solution containing an internal standard (0.02 M 4,4'-di-tert-butylbiphenyl in MeCN/DMSO 4:1, 500 µL). Aliquots (20 µL) were taken and introduced into a 96 well HPLC plate (Analytical-Sales), diluted with MeCN (700 µL) and analyzed by UPLC. Finally, data were analyzed using Virscidian Analytical Studio and results expressed as P/IS ratio using Microsoft Excel.

II. Optimization of stereoselective defluoroborylation

1. Screen 1: Reaction discovery – Variation of ligands and solvents

i. Reaction scheme:

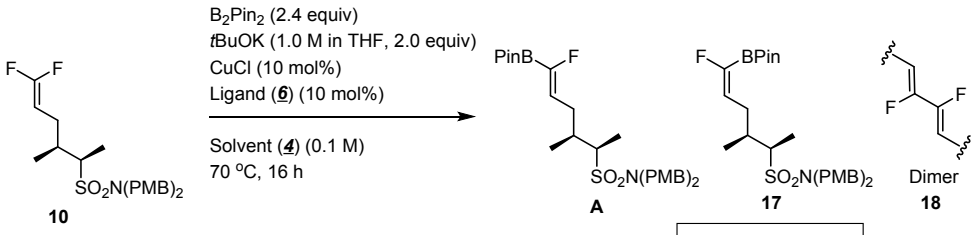

Ligand: DPEPhos, Xantphos, dppe, dFppe, DPPF, rac-Binap
Solvent: DMF, DME, THF, THF/DMF 1:1

Best results:
Xantphos in DME

ii. Rational:

At the time of our investigation, the only example of a defluoroborylation performed on an alkyl gem-difluoroalkenes was reported by Gao and Wang (single example (2u), *Adv. Synth. Catal.* **2018**, *360*, 1032-1037). In this seminal paper, DPEPhos was used as ligand and THF as solvent. The literature also suggested that ligands and solvents could have a major impact on this transformation. Therefore, we designed a first HTE screen focusing on these two parameters. We selected several bidentate phosphines known to chelate copper as well as solvents known for this transformation (THF and DMF) or known to be able to chelate Cu, providing a labile ligand as second coordination sphere.

iii. Results:

In this HTE screen, a very strong ligand effect (major parameter) as well as a solvent effect (minor parameter) were observed. Xantphos was the best ligand in terms of conversion of **10**, but also in terms of selectivity for the desired isomer (**A** vs **17**). The solvent choice appeared to influence the conversion of the reaction and selectivity between **A** and dimer **18**, but a clear rational could not be established and further screening was needed.

Screen 1: **A**/IS bar graph

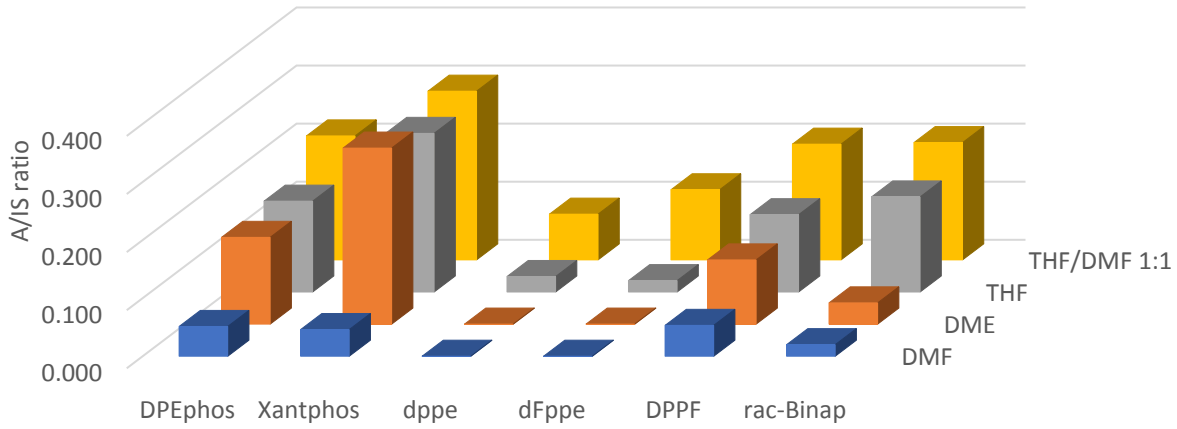

Screen 1: **10**/IS bar graph

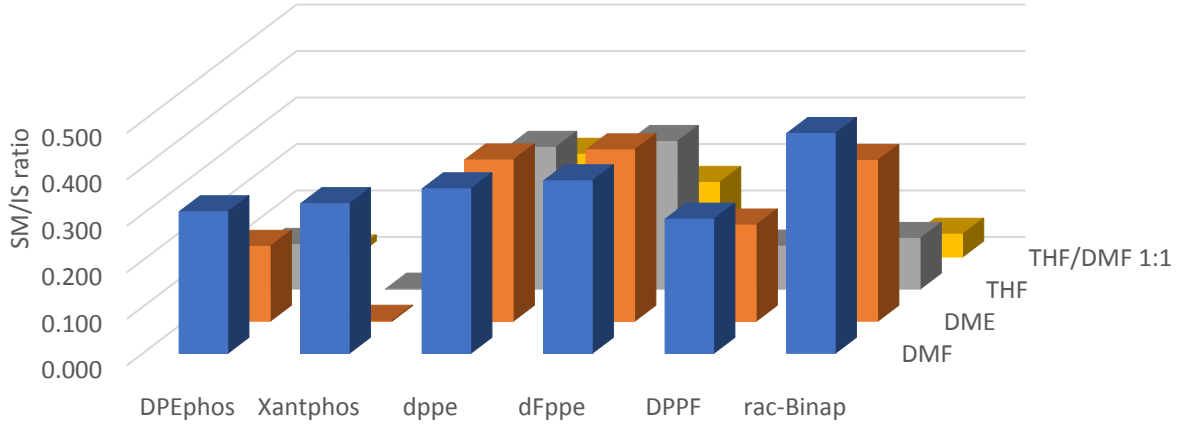

Screen 1: **A**/**17** bar graph

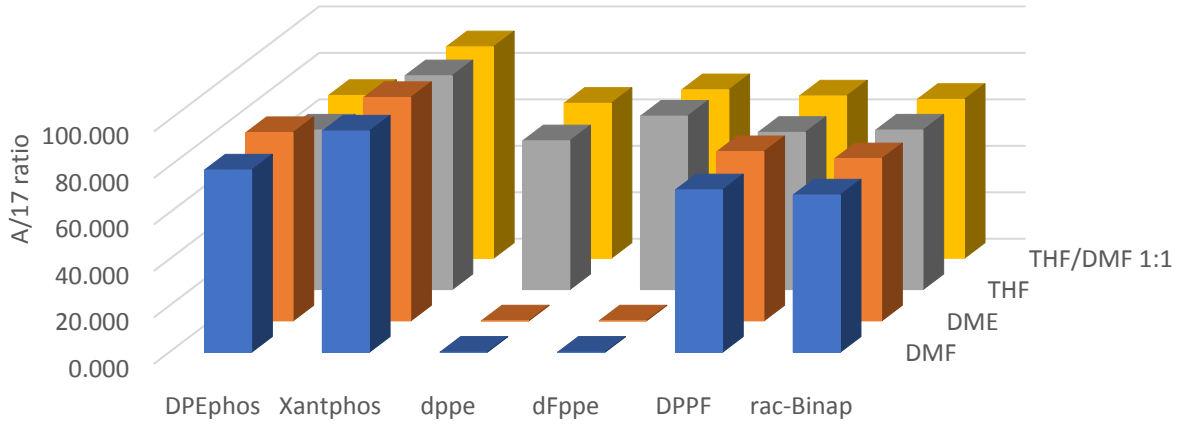

2. Screen 2: Reaction optimization – Further variation of ligands and solvents

i. Reaction scheme:

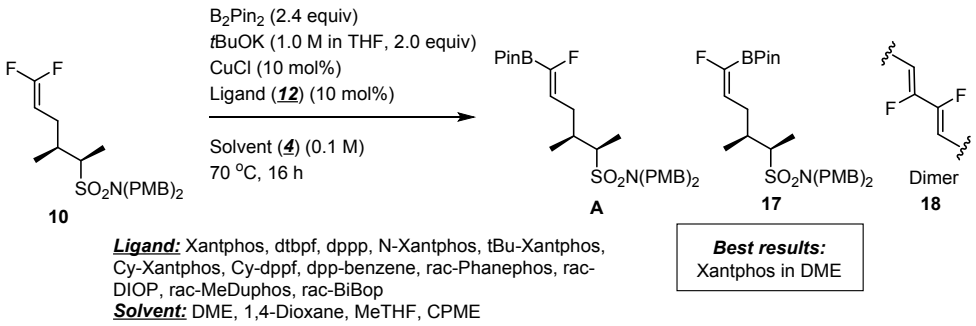

ii. Rational:

We wanted to understand how stereoelectronic parameters might affect this Cu catalyzed transformation. Therefore, we screened a large panel of ligands (major parameter) varying in bit angles, steric bulk, and electronic density. Since we noticed a solvent effect during the first HTE screen, we decided to test additional solvents (minor parameter) closely related to our best hit, DME.

iii. Results:

Again, Xantphos proved to be the best ligand. The second-best performing ligand was its structural homologue N-Xantphos. Interestingly, more electron rich analogs proved to perform poorly in this transformation with only a minor effect of the steric component (Xantphos>Cy-Xantphos~tBu-Xantphos). Conversion of **10** seemed to be corelated with the bite angle of the ligand (see *J. Chem. Soc., Dalton Trans.*, **1999**, 1519-1529; *Organometallics* **1998**, *17*, 4344-4346; *Angew. Chem. Int. Ed.* **2019**, *58*, 13573-13583), with exception of Phanephos that performed poorly in this transformation (other parameters might be involved).

Bite angle: Xantphos (107.12°) >Phanephos (103.69°) >DPEPhos (102.51°) >DIOP (97.63°) >DPPF (95.60°) >Binap (92.43°) > dppp (91.08°)>dppe (85.03°)~BiBop (85.0°) >dpp-benzene (83.04°) >DUPHOS-Me (82.61°)

P/IS of **10**: Xantphos (0.434) >DPEPhos (0.253) ~DIOP (0.250) >DPPF (0.171) > dppp (0.111) > All other ligands (only traces of product)

The solvent choice again appeared to influence the reaction profile notably in terms of selectivity **A**/**18**, with DME being the best solvent for this transformation.

Screen 2: **A**/IS bar graph

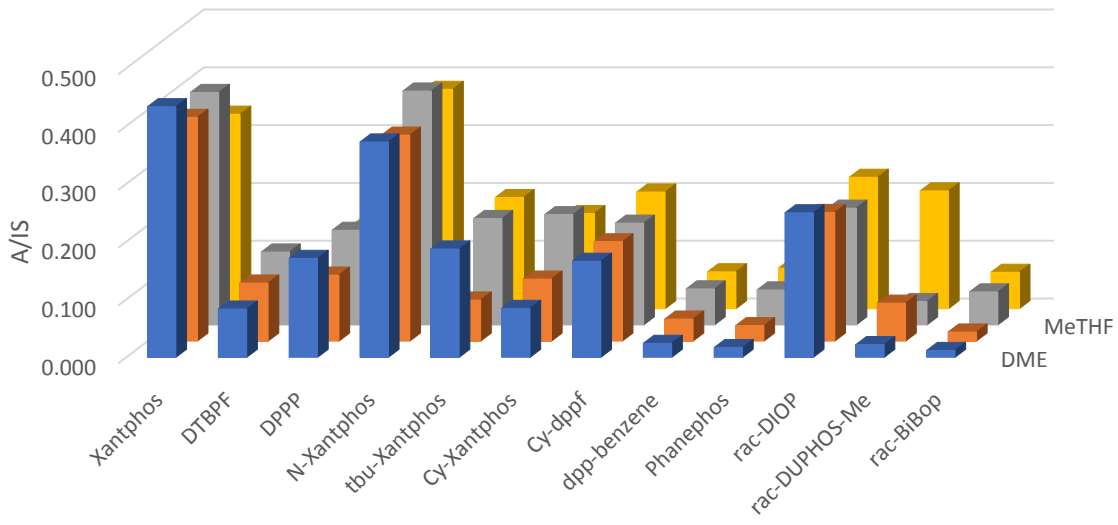

3. Screen 3. Reaction optimization – B_2Pin_2, base, and MeOH equivalents together with solvent fine tunning

   i. Reaction scheme:

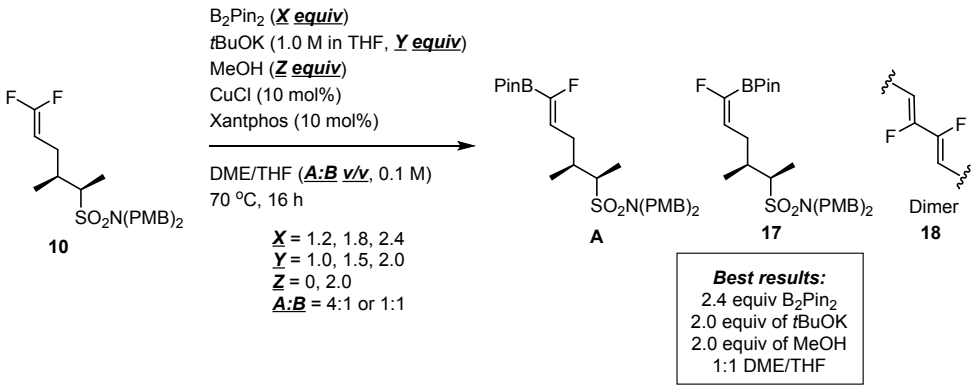

   ii. Rational:

The reaction conditions developed so far aimed to assess the effect of the ligands and solvents on this transformation without the effect of reagent starvation. The goal of this third HTE screen was to assess the necessity of the excess of all other reagents but also to fine tune the solvent system. Since *t*BuOK was used as a solution in THF, we decided to investigate the DME/THF solvent ratio.

During the course of our investigation, the group of Ito reported a very similar copper(I)-catalyzed stereoselective defluoroborylation of aliphatic gem-difluoroalkenes (*Chem. Lett*. **2018**, *47*, 1330). The authors also noticed that

Xantphos was the best ligand for this transformation. Interestingly, they noticed that MeOH was beneficial for the reaction, which prompted us to test this as an additive.

iii. Results:

An excess of base and B_2Pin_2 is necessary for the reaction to reach full conversion and the best reaction conditions happened to be the ones used in previous HTE screens (dark yellow bars, best **A**/IS indicated with a blue star, 2.4 equiv B_2Pin_2, 2.0 equiv *t*BuOK). The solvent mixture did not seem to impact the reaction, unlike MeOH that was found to be detrimental notably when using less equivalents of reagents. Interestingly, the effect of MeOH was less noticeable when using large excess of reagent (grey bars, best A/IS indicated with a red star) and the overall purity profile similar if not better to the reactions ran without MeOH (inferior conversion but reduced amount of dimer **18**).

Screen 3: **A**/IS bar graph

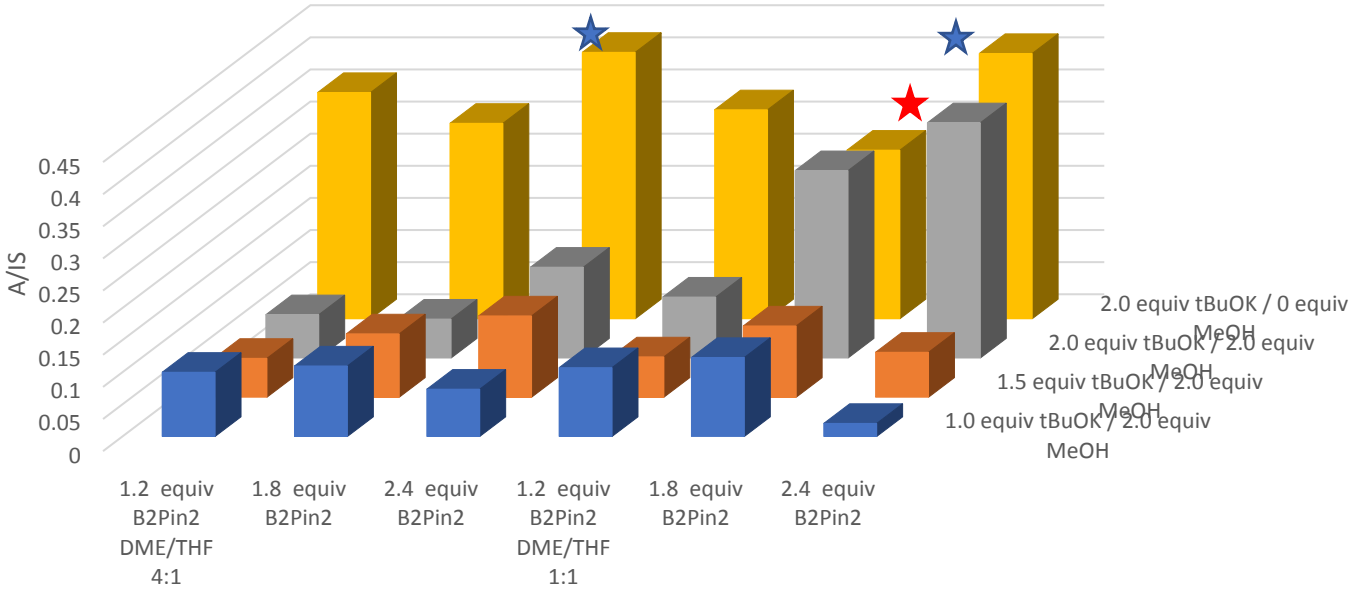

4. First benchtop scale-up

i. Reaction scheme:

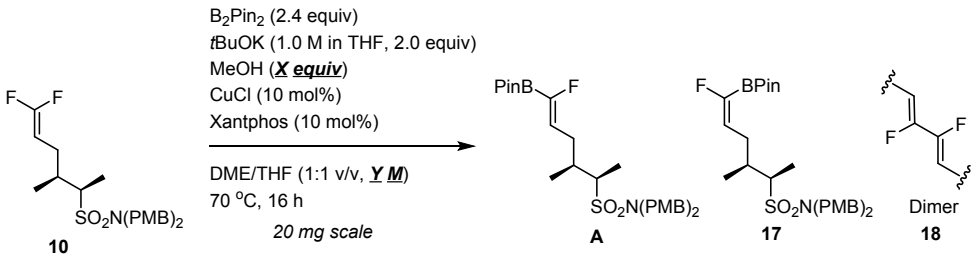

Vial 1: X = 0, Y = 0.1
Vial 2: X = 0, Y = 0.25
Vial 3: X = 2.0, Y = 0.1
Vial 4: X = 2.0, Y = 0.25

Best results: Vial 4
Increased concentration
Addition of MeOH

Vial	LCAP of **10**	LCAP of **A**	LCAP of **17**	LCAP of **18**	LCAP of all other SP
1	**ND**	**72.8**	**3.0**	**12.2**	**12.0**
2	**ND**	**72.7**	**1.9**	**18.3**	**7.1**
3	**5.1**	**85.8**	**3.4**	**2.0**	**3.7**
4	**ND**	**86.4**	**3.5**	**6.1**	**4.0**

LCAP = Liquid Chromatography Area Percent

ii. Rational:

We wanted to confirm the preliminary results on benchtop while investigating the effect of MeOH on a larger scale. We also took the opportunity to investigate the effect of the concentration on the reaction since this parameter is difficult to evaluate on HTE scale.

iii. Results:

A similar reaction profile was obtained for vial 1 compared to HTE scale, though a small increase of **18** was observed. This effect was even stronger when the reaction concentration was increased from 0.1 to 0.25 M (vial 2). As observed during HTE screening, the addition of MeOH positively affected the reaction profile (reduced amount of **18**) but slowed down the reaction and therefore **10** could be detected at EOR (vial 3). Interestingly, increasing the concentration permitted to reach full conversion of **10** to **A** with reduced amount of **18** (vial 4). These reaction conditions were used as “standard conditions” for further benchtop screening.

5. Benchtop optimization

i. Reaction scheme:

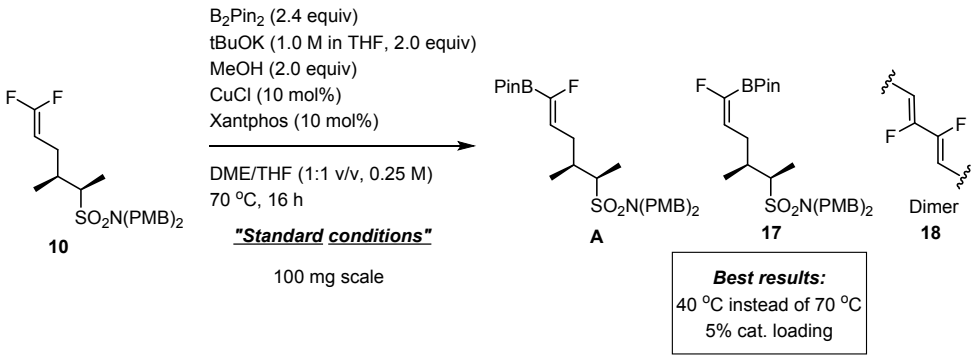

ii. Variation from standard:

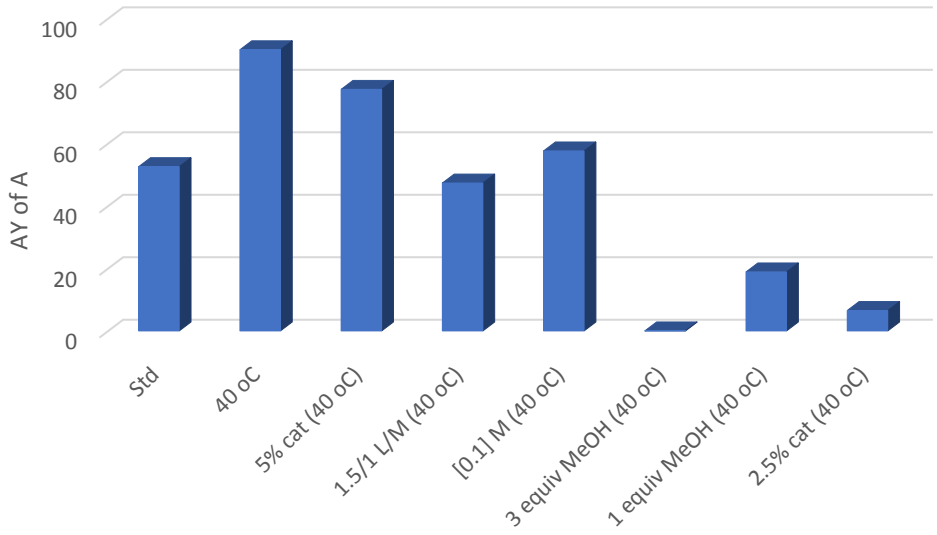

iii. Results:

Upon scale-up (20 to 100 mg), the standard conditions (Std) afforded a degraded reaction profile with a large amount of **18** being produced. We noticed a relatively strong exotherm being produced upon addition of *t*BuOK to the mixture, prompting us to lower the temperature of the reaction to 40 °C and to use a jacketed reactor (Mettler Toledo Easy Max). This modification of the procedure afforded a very similar purity profile than those obtained on HTE scale, yielding **A** in 90% AY. As expected, lowering the catalyst loading to 5 mol% slowed down the reaction but surprisingly, almost no reaction was observed with 2.5 mol% of catalyst, suggesting a catalyst poisoning. In order to circumvent this side reaction, more ligand was added (1.5:1 L/M ratio), but this only further slowed down the reaction.

6. Final conditions

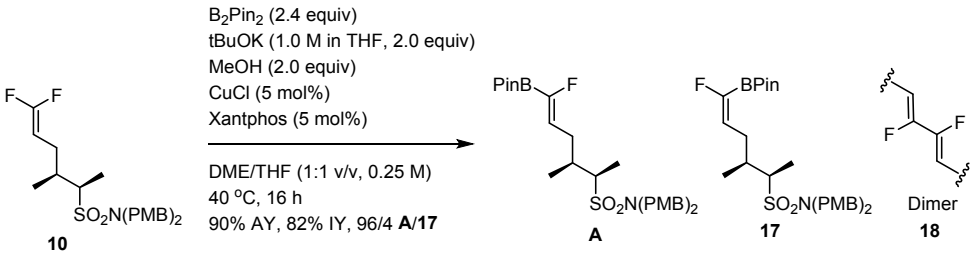

Finally, our best conditions (see manuscript) where obtained by performing a slow addition of *t*BuOK to the reaction mixture. Thus, any exothermic reaction or catalyst deactivation could be avoided, allowing us to drop the catalyst loading to 5 mol% while still reaching full conversion of **10**.

III. Scale up of nucleophilic opening of cyclic sulfate **2**

The investigation of the reaction between cyclic sulfate **2** and trifluoropropylmagnesium chloride **12** revealed that both the ring opening and the seemingly straightforward desulfation contributed to the low yield of the alcohol formation. We monitored the formation of the intermediate via QNMR study. The results indicated that the open sulfate (intermediate **53B**) was formed in 43% AY, though the final product was only isolated in 26% IY after hydrolysis. This observation prompted us to investigate the ring opening of epoxide **11** since the troublesome hydrolysis could be avoided, directly affording the desired alcohol **9**.

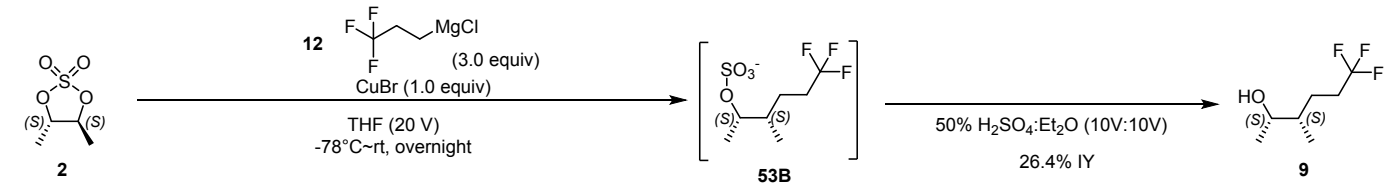

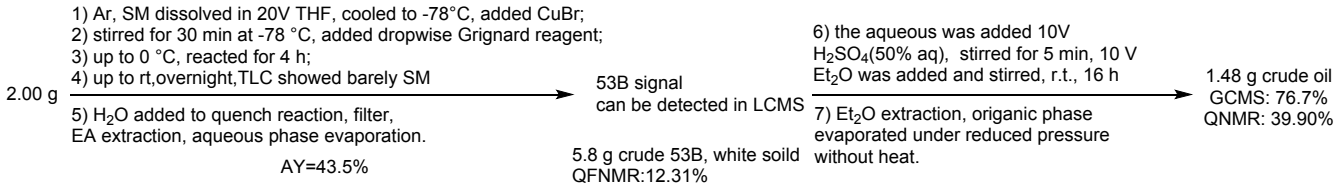

IV. Nucleophilic opening of epoxide **11**

The nucleophilic opening of epoxide **11** was reported in the literature using allylmagnesium chloride or bromide (*Tetrahedron* **1990**, *46*, 4503-4516; *Org. Biomol. Chem.* **2015**, *28*, 7813-7821). After our setback with sulfate **2**, we

applied the optimized conditions (3.0 equiv of Grignard with stoichiometric CuBr in THF) found for the opening of **2** to **11** and were delighted to obtain the targeted alcohol **9** in very high AY (see manuscript). We then directly applied the literature conditions (3.0 equiv of Grignard with catalytic CuI in THF) and obtained alcohol **9** in 75% AY and 7:1 *dr*. Further refinement showed that a smaller excess of Grignard (2.0 equiv) afforded similar AY and purity profiles.

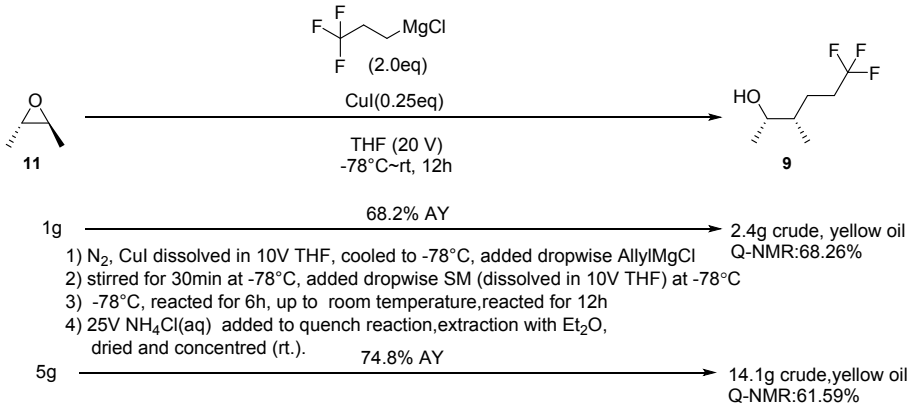

V. Installation of sulfur atom on the fragment

1. Alternative disconnections to Mitsunobu

The patent literature (PCT Int. Appl. WO 2016033486) showed the installation of the sulfur atom on the chain via a lengthy Mitsunobu/ oxidation/ hydrolysis sequence. We aimed to develop a shorter route avoiding this poorly atom economic transformation, therefore we scooted various disconnections.

i. Activation then SN2:

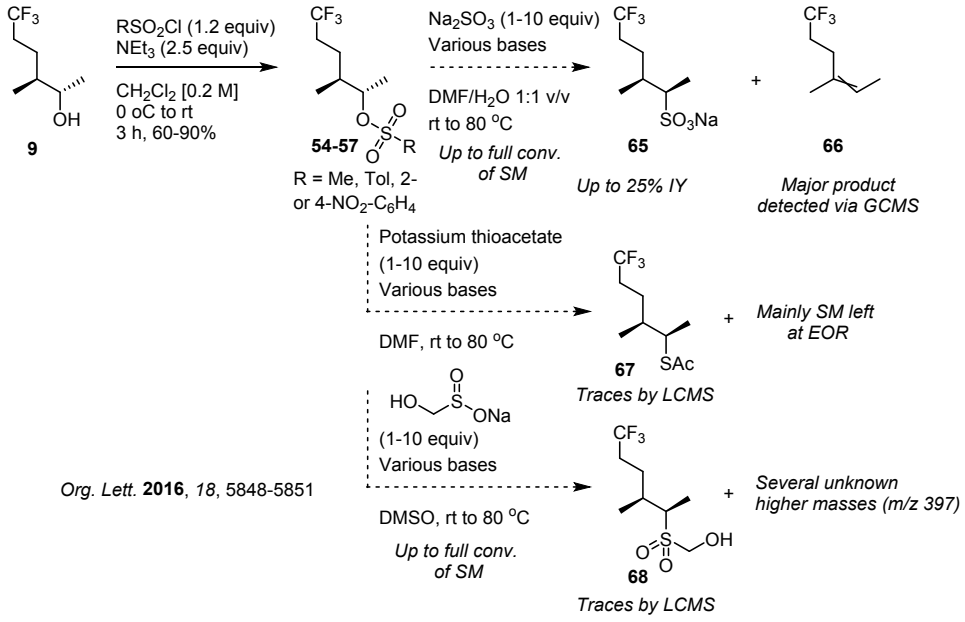

ii. SN2 with in situ generated sulfur ylide:

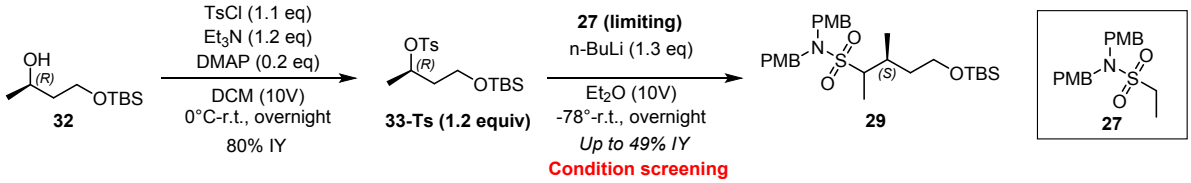

Condition screening:

Entry	Base	CuX	Solvent	Result (Area% in 210nm)		
				SM (**27**)	P (**29**)	SP: m/z:340
1	n-BuLi	-	Et_2O	9.6%	51.1% (49% IY)	-
2	n-BuLi	CuI	Et_2O	24.6		-
3	n-BuLi	CuBr	Et_2O	25.3%	4.9%	-
4	n-BuLi	-	Toluene	10.2%	48.5%	-
5	n-BuLi	CuI	Toluene	14.6%	24.2%	-
6	n-BuLi	CuBr	Toluene	14.9%	11.0%	-
7	n-BuLi	-	MTBE	12.7%	46.1%	-
8	LDA	-	THF	16.3%	11.1%	23.5%
9	LDA	-	Et_2O	18.4%	22.9%	27.6%
10	LDA	-	Toluene	15.2%	26.6%	23.0%
11*	KHMDS	-	THF	No reaction, major SM (* 0 °C overnight)		
12*	kHMDS	-	Et_2O	No reaction, major SM (* 0 °C overnight)		
13	CyclohexylMgBr	-	Et_2O	69.4%	-	-
14	CyclohexylMgBr	-	THF	81.8%	-	-
15	CyclohexylMgBr	-	Toluene	78.9%	-	-
16	MeMgBr	-	Et_2O	57.4%	-	1.6%
17	MeMgBr	-	THF	65.7%	-	-
18	MeMgBr	-	Toluene	61.4%	-	-
19	$(C_4H_9)_2Mg$	-	Et_2O	30.4%	15.9%	16.6%
20	$(C_4H_9)_2Mg$	-	THF	41.7%	15.2%	-
21	$(C_4H_9)_2Mg$	-	Toluene	30.4%	9.1%	25.2%

2. Mitsunobu optimization

With the results from the alternative disconnections being deceiving, we decided to test alternative reaction conditions for the Mitsunobu step. Our best results were obtained by lowering the excess of thiopyrimidine from 2.3 equiv (original report on alkenyl derivative) to 1.0 equiv. Alternative reagents were also tested, without success.

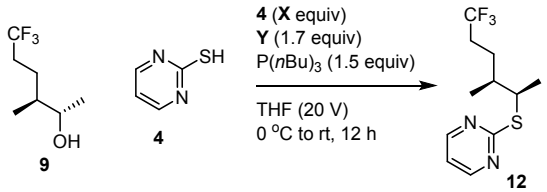

Y = DEAD, X = 2.3 equiv, 42% AY
Y = DEAD, X = 1.0 equiv, 72% IY, >200:1 *dr*
Y = Tsunoda reagent, X = 2.3 equiv, **12** not detected
Y = DIAD, X = 2.3 equiv, **12** not detected

VI. Base mediated defluorination of alkyl trifluoromethyl to gem-difluoro alkyl

We examined the defluorination reaction for various substrates containing a trifluoromethyl group, including **9**, **12** and the trifluoromethyl analogue of **14** and **15** (**14'** and **15'**, respectively). Substrates **9** and **12** were rapidly found to be the most promising substrates for such eliminations and both substrates were further investigated. On the contrary, the defluorination completely failed with **14'** and **15'**.

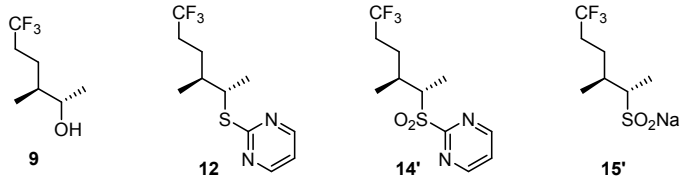

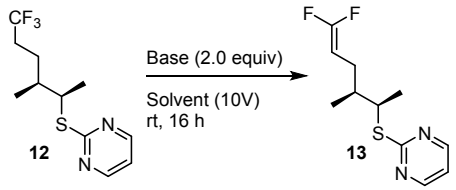

Entry	Solvent (10V)	Base (2.0equiv)	Result (210nm, %)	
			12	**13**
1	DMF	*t*-BuOK	9.70	16.6
2	DMF	DBU	88.3	0
3	DMF	LDA	33.9	0
4	DMF	TEA	84.7	0
5	DMF	KHDMS	0	89.00% (76% IY)

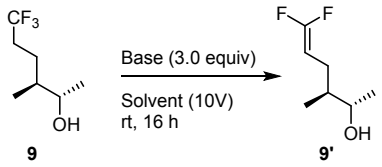

Entry	Solvent (10V)	Base (3.0 equiv)	Result(GCMS, %)		
			9'	**9**	other
1	THF	KHDMS	16.7	10.9	72.4
2	Et_2O	KHDMS	37.2	18.5	44.3
3	DMF	KHDMS	54.4	5.0	40.6
4	DME	KHDMS	30.4	12.9	56.7
5	DMF	*t*-BuOK	0	0	29.4
6	THF	KH	0	0	38.2
7	THF	KHDMS,18-crown-6	46.7	15.1	7
8	THF	Cyclohexyl-MgBr	0	12.3	75
9	THF	Dibutyl-Mg	12.1	35.0	24.3

The optimization on intermediate **9** led to conditions employing KHMDS as the base in presence of 18-crown-6-ether as additive. Considering the poorer reaction profile, toxicity, and price of this additive, we determined **12** to be a more suitable substrate for the defluorination step. Moreover, **9'** was found to be a poor partner in the Mitsunobu reaction, affording a complex mixture of products.

Treatment of **12** with 2 equivalents of KHMDS in DMF afforded **13** in 76% IY. Though only product could be detected via LCMS, the reaction suffered from an impaired mass balance. We assumed that oxidation might occur readily, which explains why we used crude **13** in the oxidation step.

VII. Alternative *S-N* bond forming reaction

The targeted intermediate **A** possesses a bis-PMB protected sulfonamide group installed via a S-N bond forming reaction using hydroxylamine-*O*-sulfonic acid (HOSA) as aminating reagent. We envisioned to avoid this expensive and toxic reagent while shortening the synthesis by the direct installation of bis-PMB amine. Unfortunately, no reaction affording the targeted product could be found.

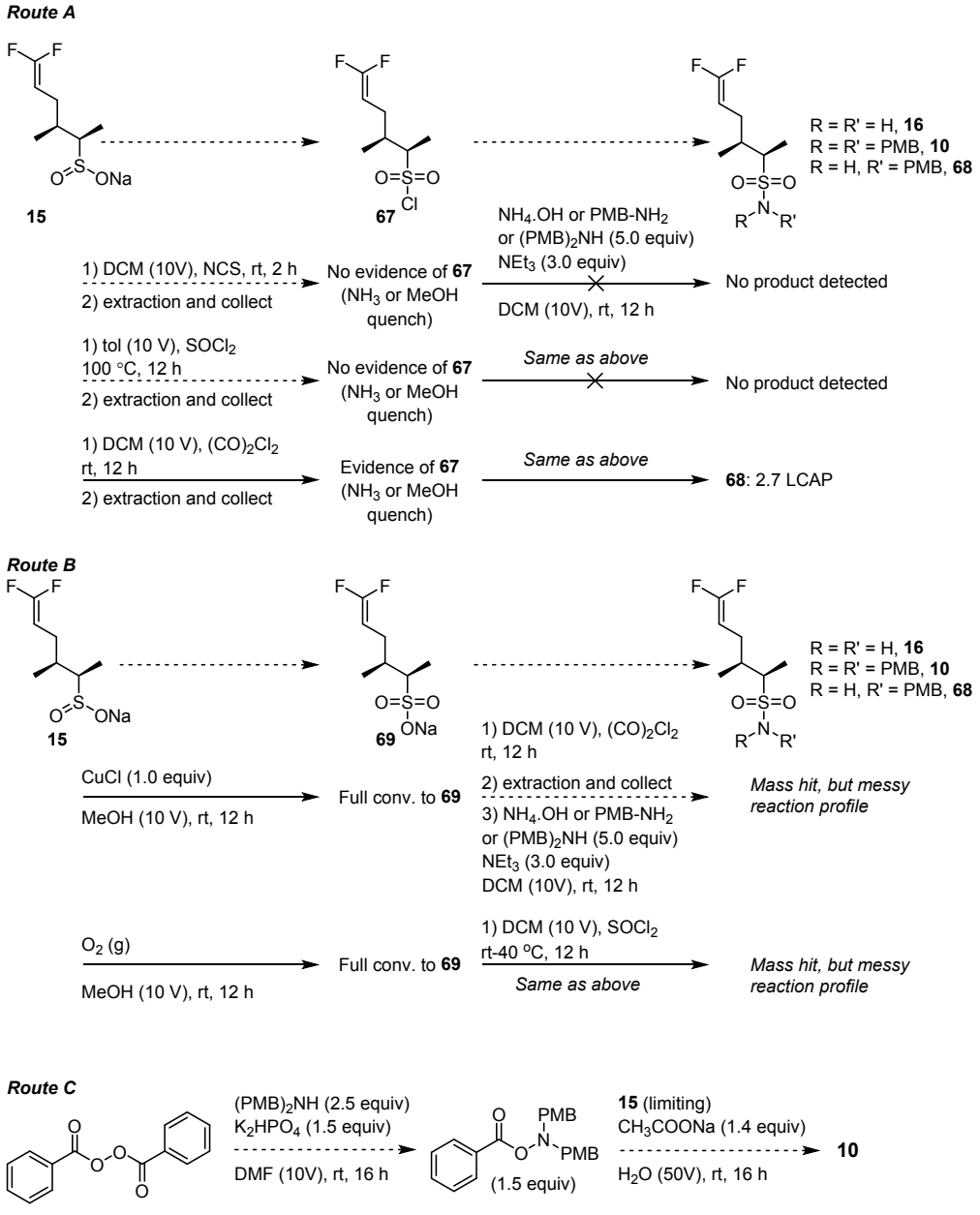

VIII. HRMS Analysis

The liquid chromatography (LC) experiments were performed using an Ultimate 3000 RS UHPLC system (Thermo Fisher Scientific) composed of a gradient pump, an autosampler, a column oven, and a diode-array detector (DAD). DAD scanning wavelength: 210 to 400 nm. Mobile phase A: 0.1% ammonium bicarbonate in 95% H_2O + 5% CH_3CN; Mobile phase B: CH_3CN. Column: Acquity UPLC BEH C18, 2.1 mm i.d. x 100 mm, 1.7 um (Waters Corporation). The LC experiments were carried out at 55 °C and at a flow rate of 0.6 mL/min applying a linear gradient from 95% A to 5% A in 2.10 min and held for 1.9 min. A 1:10 flow split from the column to the MS spectrometer was applied.

The HRMS experiments were performed in Full MS scan type mode on a Q-Exactive mass spectrometer (Thermo Fisher Scientific) with electrospray ionization (ESI) and using nitrogen as carrier gas. The MS was calibrated in both positive and negative modes according to the manufacturer instructions prior to any measurement. ESI parameters: spray voltage: 4.00 kV; capillary temperature: 320 °C; S-lens RF level: 50.0. Masses *m/z* ranging 100 to 1200. Xcalibur (version 4.4, Thermo Fisher Scientific) was used as data acquisition software.

IX. NMR Spectra

1. Staged intermediates

^{1}H NMR (400 MHz, Chloroform-*d*) of 2-(((2*R*,3*S*)-6,6,6-trifluoro-3-methylhexan-2-yl)thio)pyrimidine (**12**)

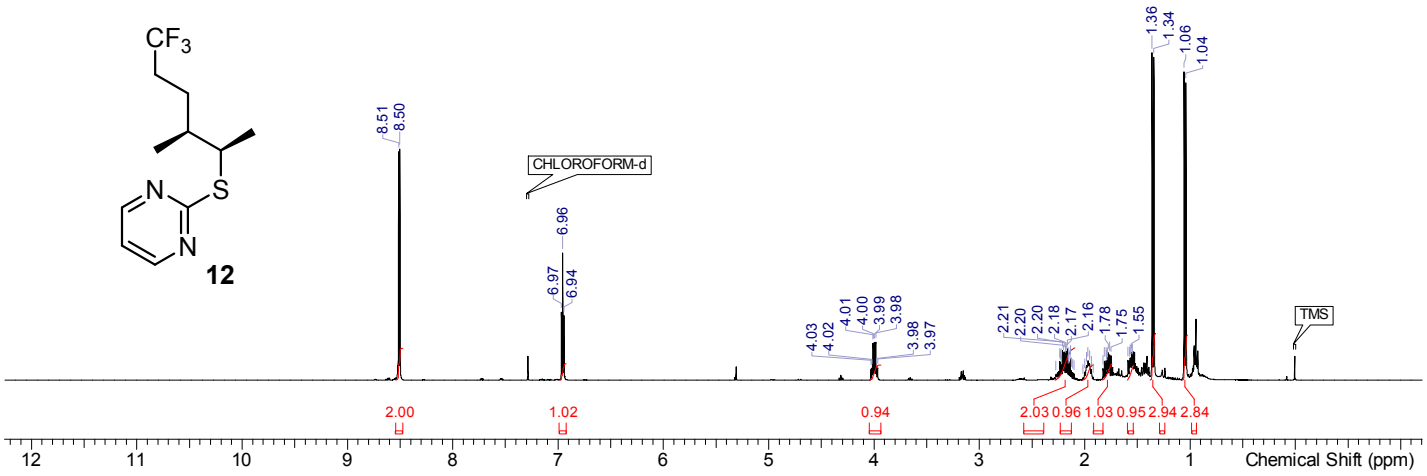

^{13}C {^{1}H} NMR (101 MHz, Chloroform-*d*) of 2-(((2*R*,3*S*)-6,6,6-trifluoro-3-methylhexan-2-yl)thio)pyrimidine (**12**)

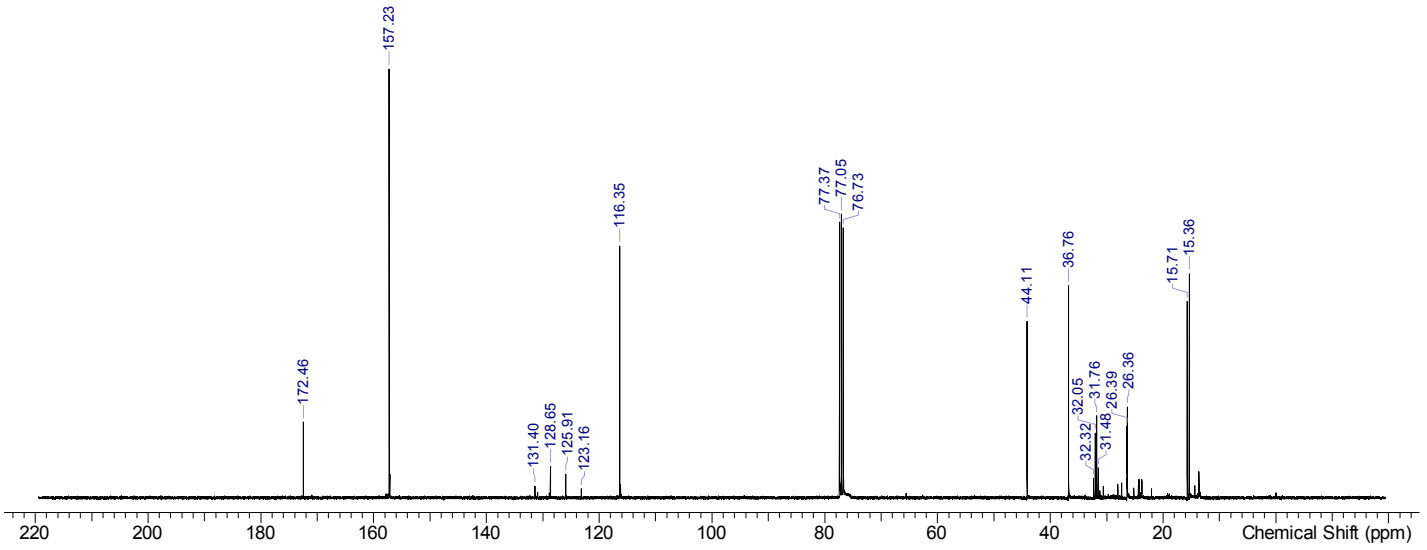

^{19}F {^{1}H} NMR (376 MHz, Chloroform-*d*) of 2-(((2*R*,3*S*)-6,6,6-trifluoro-3-methylhexan-2-yl)thio)pyrimidine (**12**)

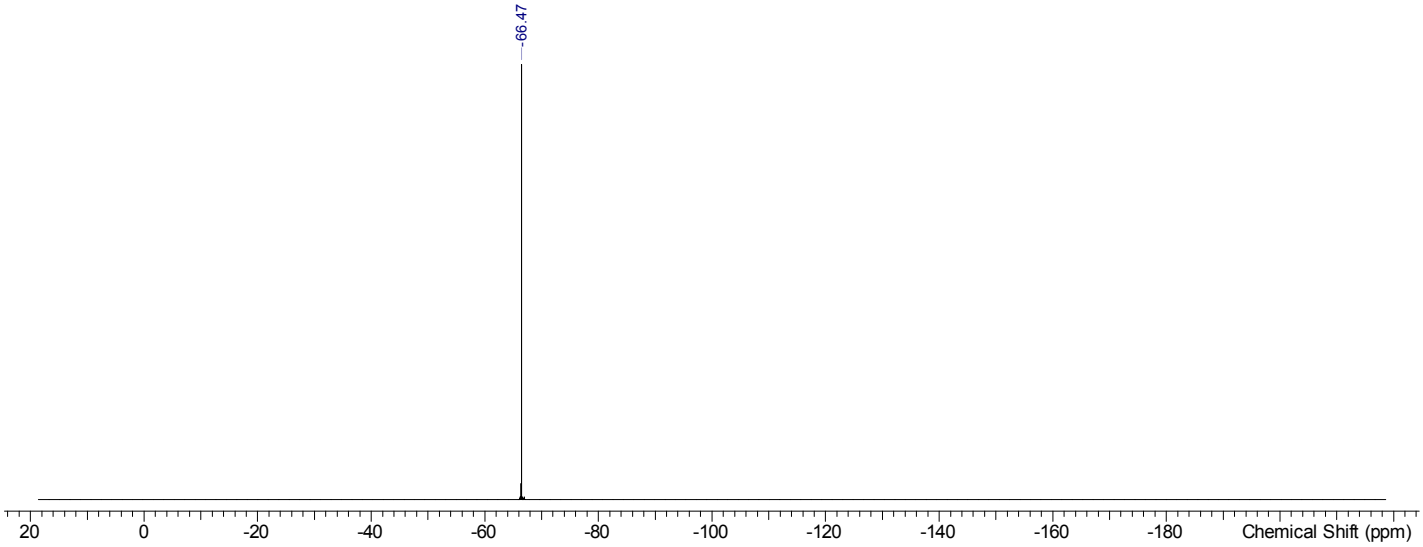

UPLC spectra of 2-(((2*R*,3*S*)-6,6,6-trifluoro-3-methylhexan-2-yl)thio)pyrimidine (**12**)

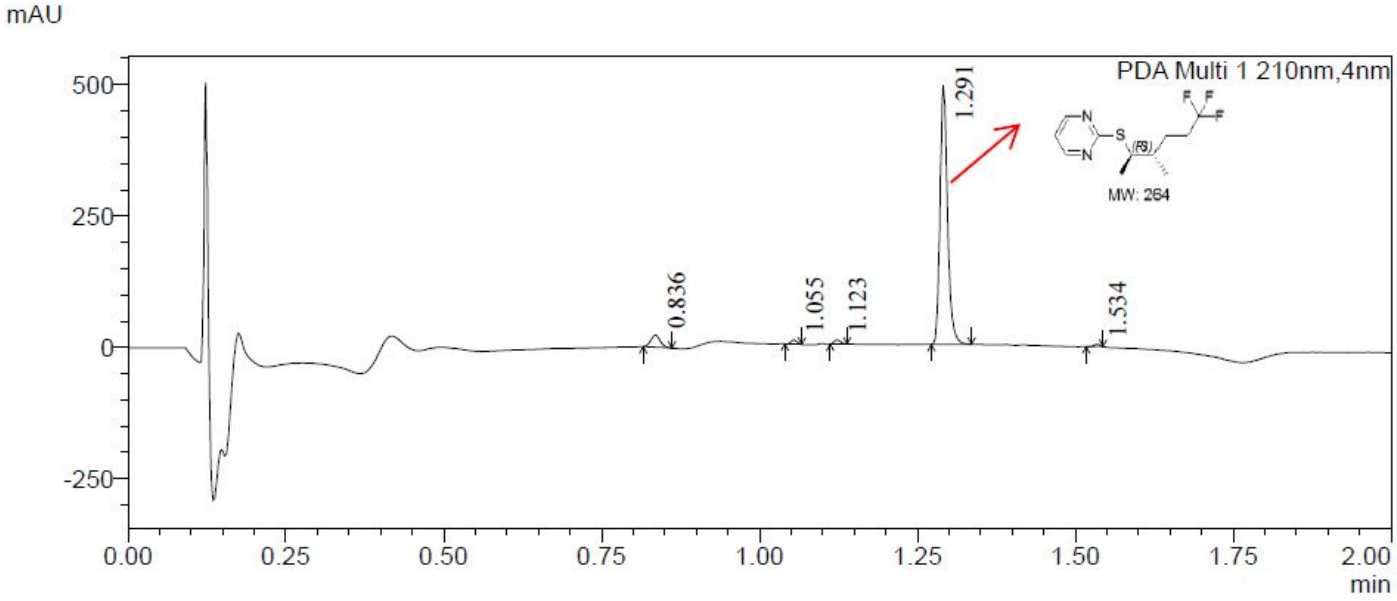

Peak Table

PDA Ch1 210nm

Peak#	Ret. Time	Height	Height%	Area	Area%
1	0.836	22626	4.386	23433	5.292
2	1.055	7403	1.435	4664	1.054
3	1.123	7894	1.530	5573	1.259
4	1.291	473536	91.797	406449	91.800
5	1.534	4394	0.852	2635	0.595
Total		515853	100.000	442755	100.000

Chiral HPLC spectra of 2-(((2*R*,3*S*)-6,6,6-trifluoro-3-methylhexan-2-yl)thio)pyrimidine (**12**)

Sample Name : JPNV-BE043-55-104-4(52313-001P1)1T
Data File : D:\LC83DATA\data\2020data\202010\20201028\001 2020-10-28 11-16-04
Injection Date : 10/28/2020 4:44:26 AM
Injection Volume : 2.0 µL
Acq. Method : Chiral-4.M
Column Name : CHIRAL Cellulose-SB4.6*100 mm 3 µm
Method Comment : Mobile phase : Hex(0.1%DEA):IPA=98:2
Flow : 1.0 ml/min
Temperature : 25°C
Instrument : Agilent 1260(LC83)

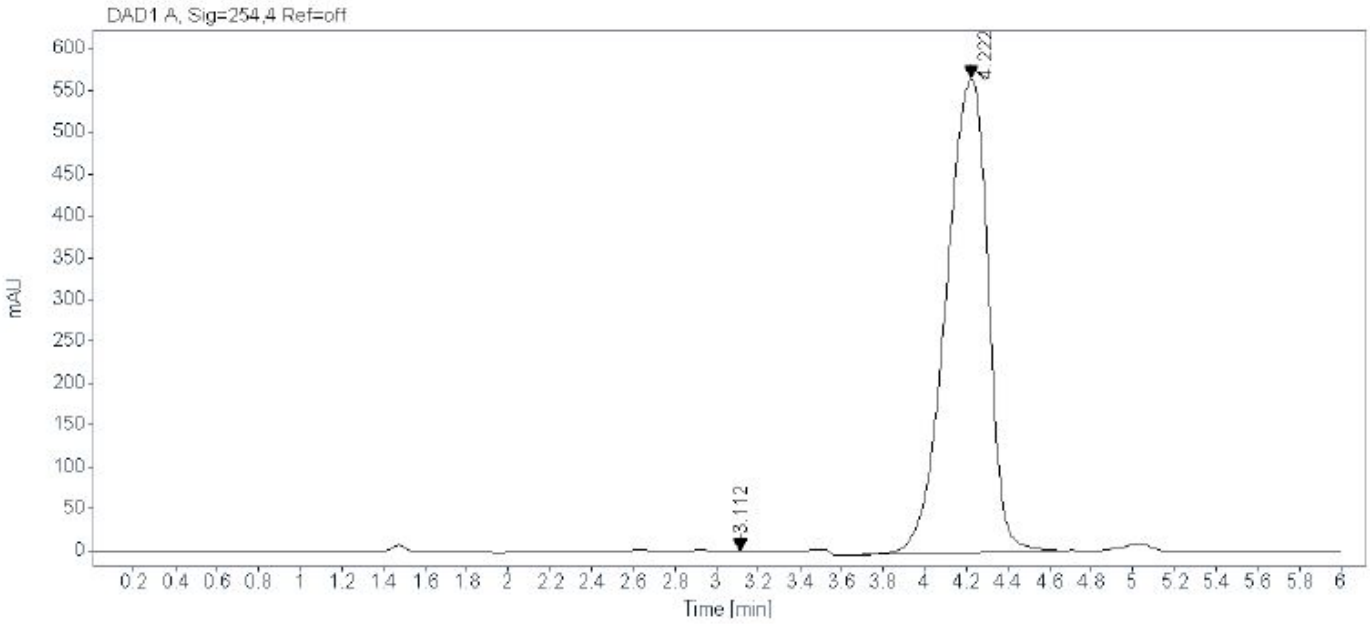

Signal: DAD1 A, Sig=254,4 Ref=off

RT [min]	Area	Height	Area%	Peak Resolution USP
3.11	2.88	0.71	0.036	
4.22	7963.40	568.00	99.964	4.76
Sum	7966.2722			

Chiral HPLC of ***cis/trans* mixture** of 2-((-6,6,6-trifluoro-3-methylhexan-2-yl)thio)pyrimidine

Sample Name	: JPNV-BE043-55-104-4(52313-001P2)1T
Data File	: D:\LC83DATA\data\2020data\202010\20201028\001 2020-10-28 11-16-04
Injection Date	: 10/28/2020 5:11:14 AM
Injection Volume	: 0.1 µL
Acq. Method	: Chiral-4.M
Column Name	: CHIRAL Cellulose-SB4.6*100 mm 3 µm
Method Comment	: Mobile phase : Hex(0.1%DEA):IPA=98:2 Flow : 1.0 ml/min Temperature : 25°C
Instrument	: Agilent 1260(LC83)

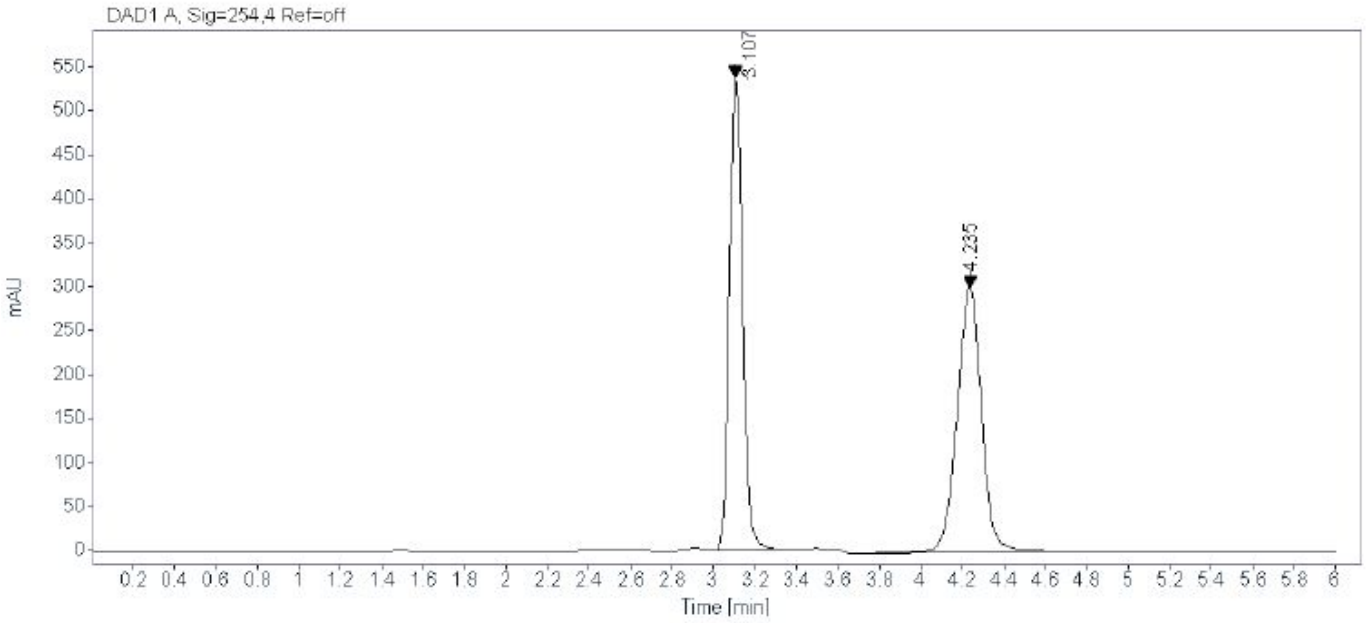

Signal: DAD1 A, Sig=254,4 Ref=off

RT [min]	Area	Height	Area%	Peak Resolution USP
3.11	2359.30	538.86	48.445	
4.24	2510.79	301.42	51.555	6.95
Sum	4870.0867			

^{1}H NMR (300 MHz, Chloroform-*d*) of 2-(((2*R*,3*S*)-6,6-difluoro-3-methylhex-5-en-2-yl)sulfonyl)pyrimidine (**14**)

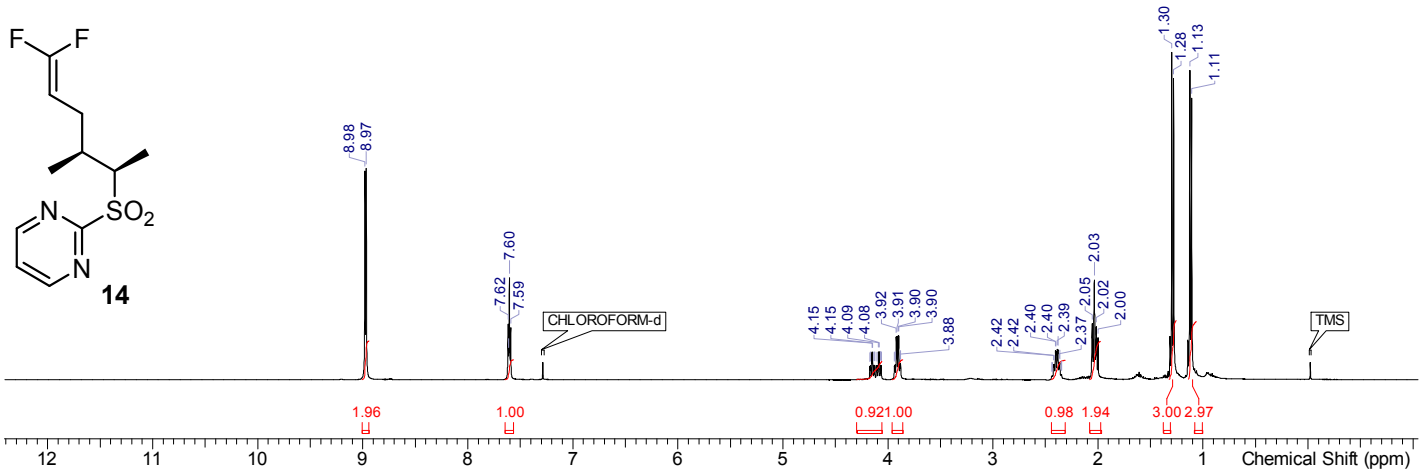

^{13}C {^{1}H} NMR (101 MHz, Chloroform-*d*) of 2-(((2*R*,3*S*)-6,6-difluoro-3-methylhex-5-en-2-yl)sulfonyl)pyrimidine (**14**)

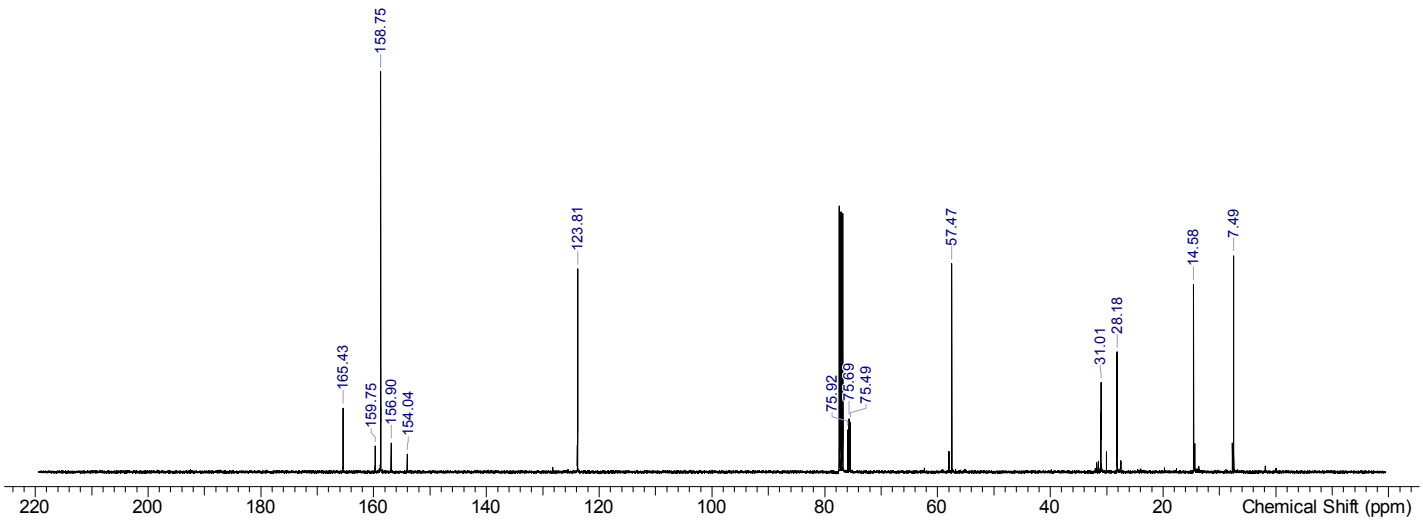

^{19}F {^{1}H} NMR (376 MHz, Chloroform-*d*) of 2-(((2*R*,3*S*)-6,6-difluoro-3-methylhex-5-en-2-yl)sulfonyl)pyrimidine (**14**)

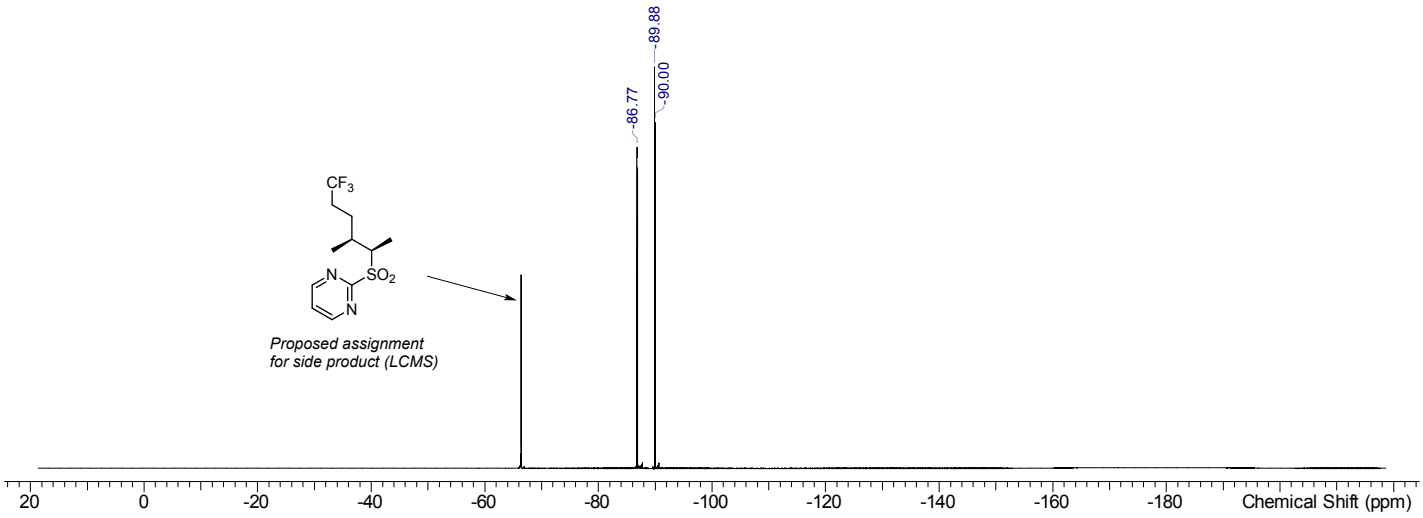

Chiral HPLC spectra of 2-(((2*R*,3*S*)-6,6-difluoro-3-methylhex-5-en-2-yl)sulfonyl)pyrimidine (**14**)

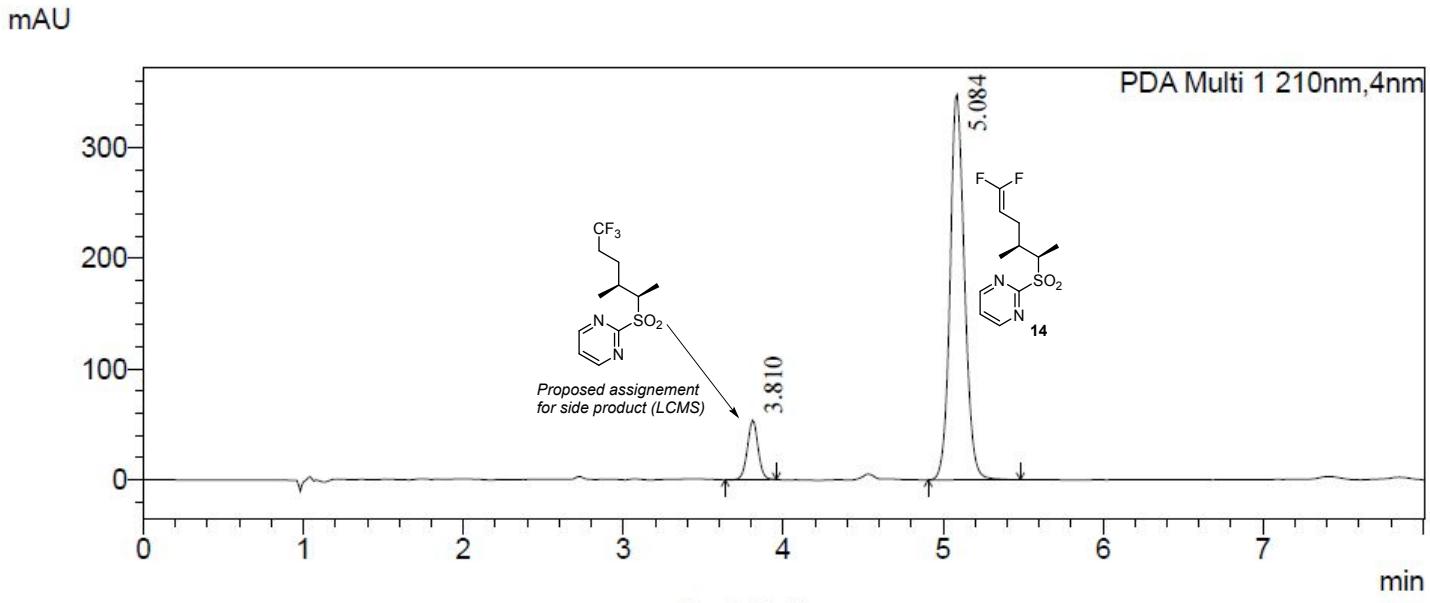

Peak Table

PDA Ch1 210nm

Peak#	R.T	Width(50%)	Height	Area	Area%
1	3.81	0.071	53582.9	249919.0	10.25
2	5.08	0.095	348147.5	2187197.1	89.75
Total			401730.4	2437116.0	100.00

Chiral HPLC spectra of ***cis*/*trans* mixture** of 2-((-6,6-difluoro-3-methylhex-5-en-2-yl)sulfonyl)pyrimidine

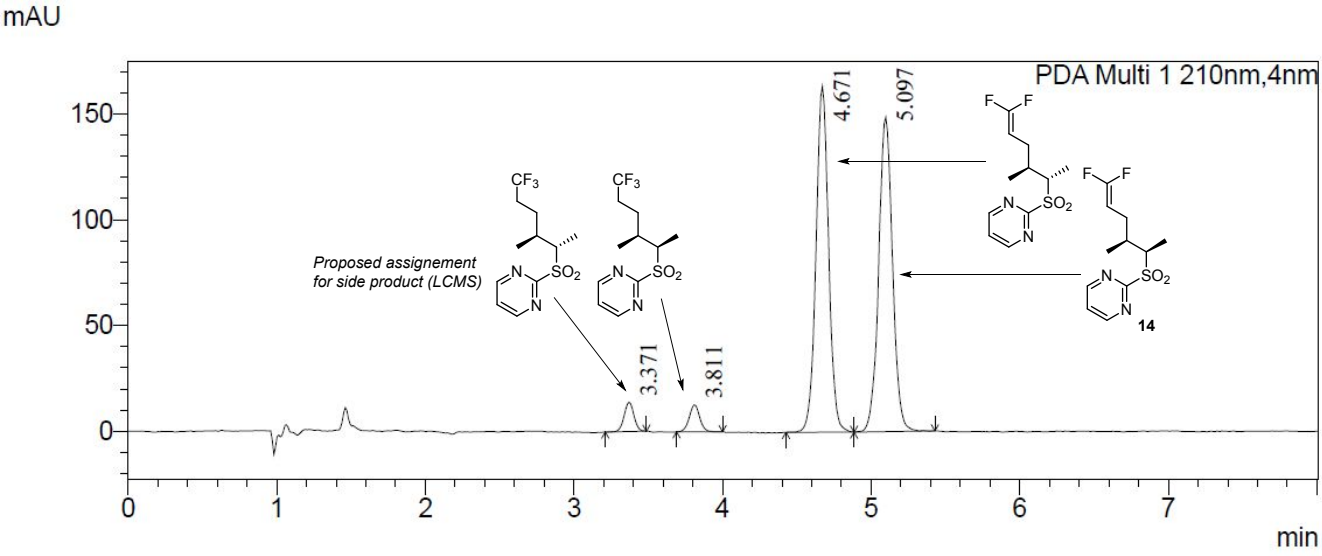

Peak Table

PDA Ch1 210nm

Peak#	R.T	Width(50%)	Height	Area	Area%
1	3.37	0.071	13918.7	64052.7	3.11
2	3.81	0.075	12723.4	62449.7	3.04
3	4.67	0.089	163608.0	965681.5	46.93
4	5.10	0.098	148805.4	965452.2	46.92
Total			339055.5	2057636.1	100.00

^{1}H NMR (400 MHz, Chloroform-*d*) of (2*R*,3*S*)-6,6-difluoro-3-methylhex-5-ene-2-sulfonamide (**16**)

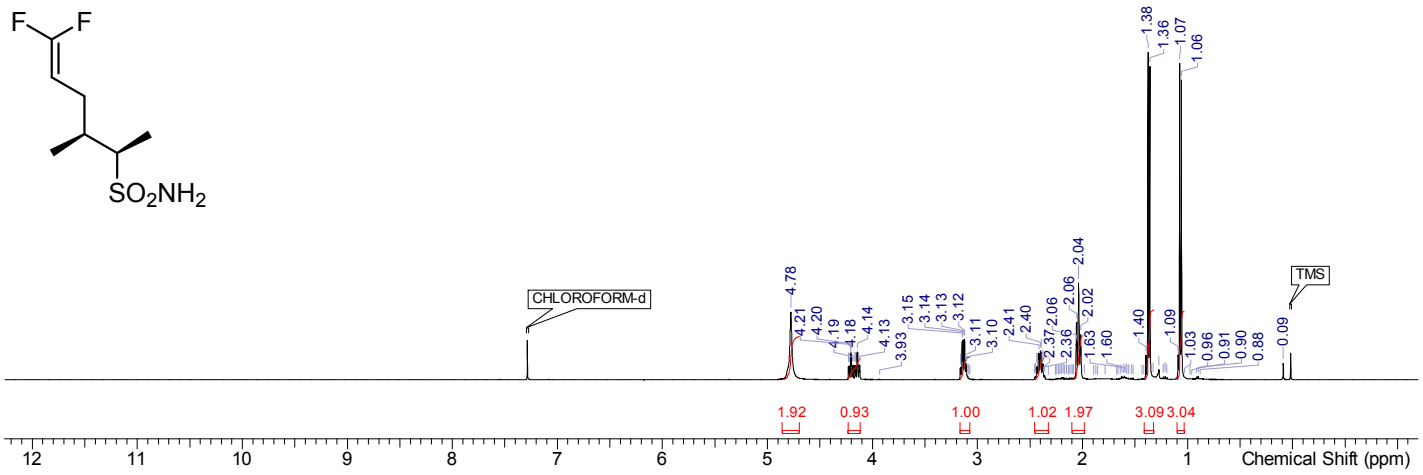

^{13}C {^{1}H} NMR (101 MHz, Chloroform-*d*) of (2*R*,3*S*)-6,6-difluoro-3-methylhex-5-ene-2-sulfonamide (**16**)

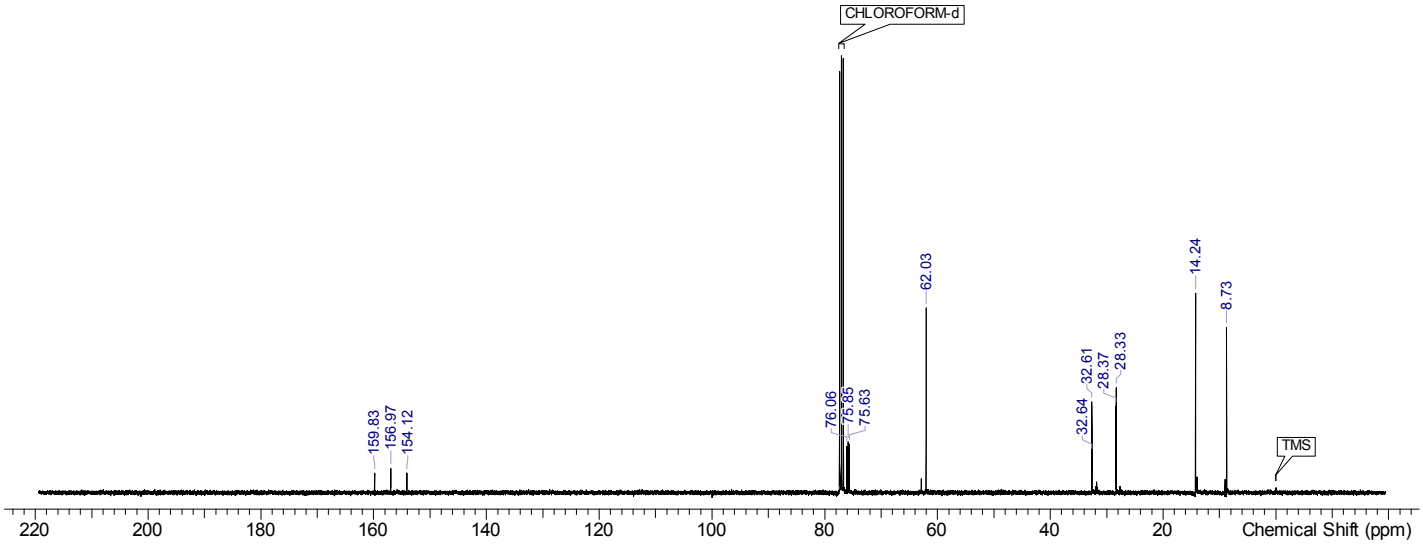

^{19}F {^{1}H} NMR (376 MHz, Chloroform-*d*) of (2*R*,3*S*)-6,6-difluoro-3-methylhex-5-ene-2-sulfonamide (**16**)

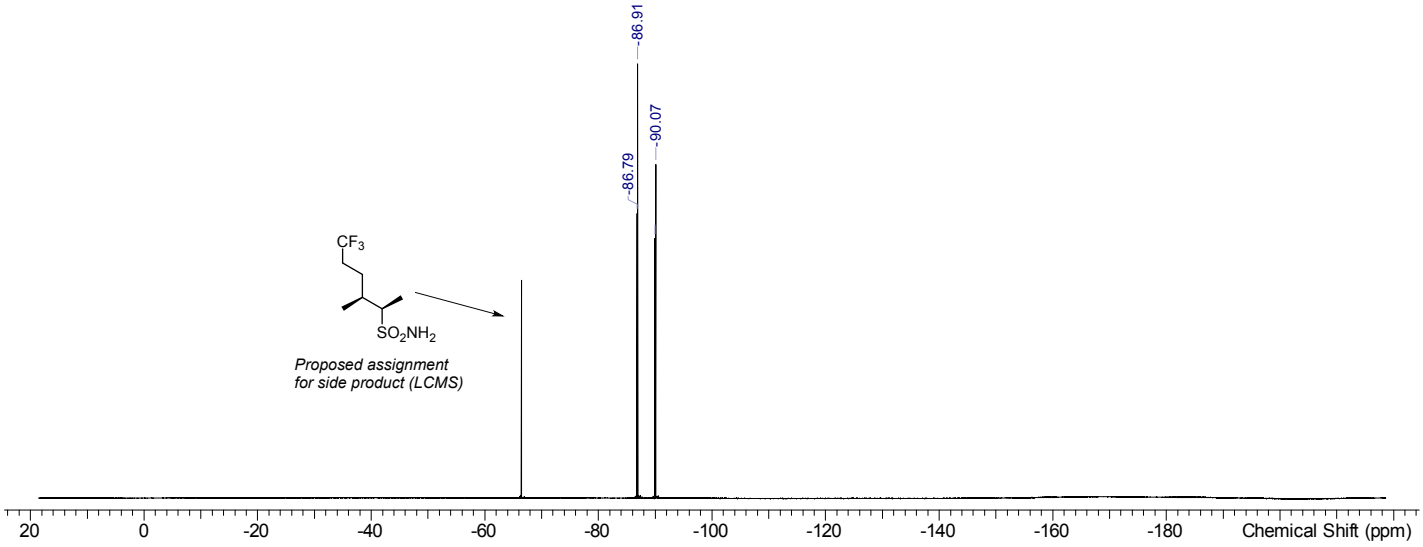

^{1}H NMR (400 MHz, Chloroform-*d*) of (2*R*,3*S*)-6,6-difluoro-*N*,*N*-bis(4-methoxybenzyl)-3-methylhex-5-ene-2-sulfonamide (**10**)

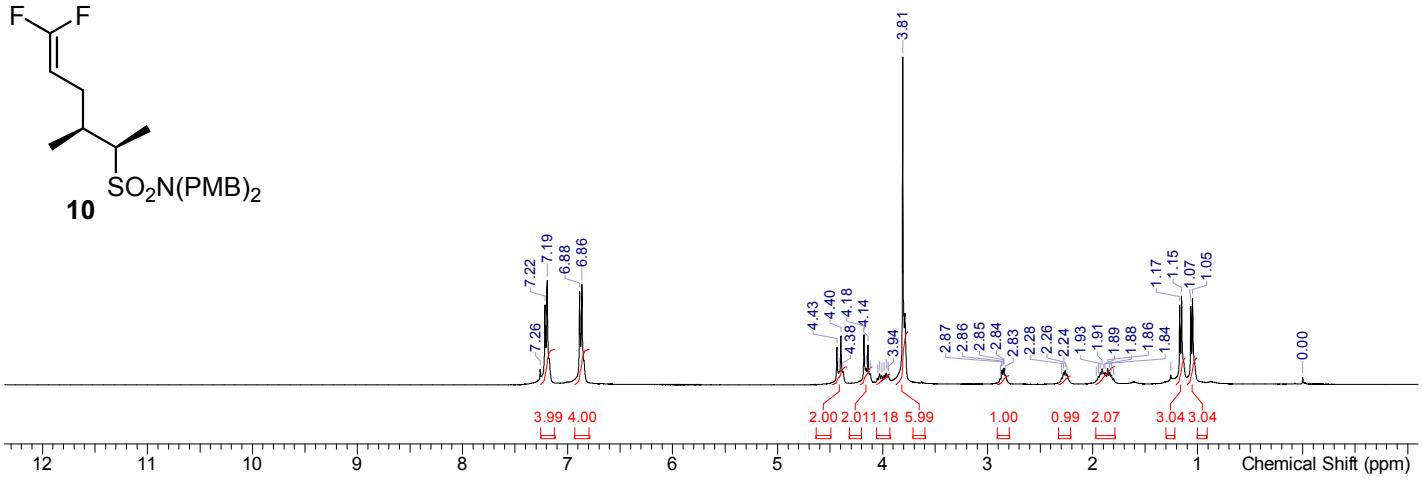

^{13}C {^{1}H} NMR (101 MHz, Chloroform-*d*) of (2*R*,3*S*)-6,6-difluoro-*N*,*N*-bis(4-methoxybenzyl)-3-methylhex-5-ene-2-sulfonamide (**10**)

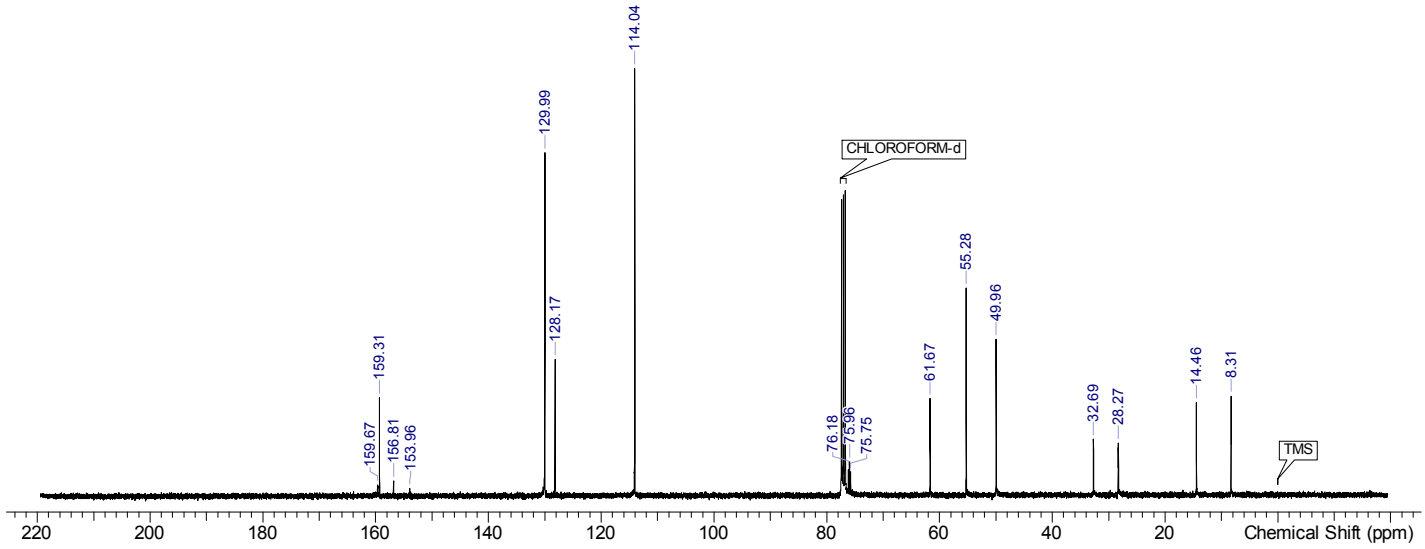

^{19}F {^{1}H} NMR (376 MHz, Chloroform-*d*) of (2*R*,3*S*)-6,6-difluoro-*N*,*N*-bis(4-methoxybenzyl)-3-methylhex-5-ene-2-sulfonamide (**10**)

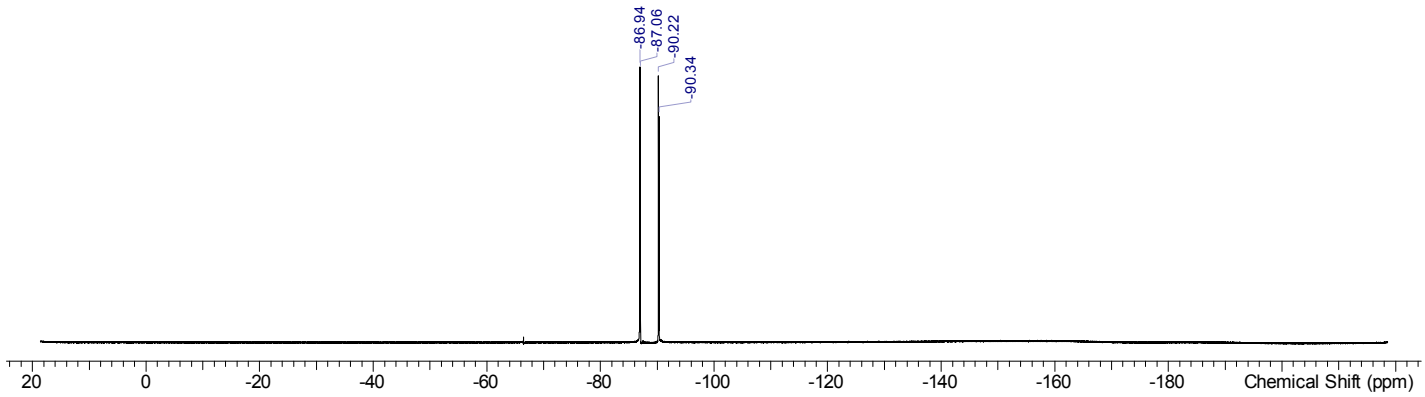

^{1}H NMR (400 MHz, Chloroform-*d*) of (2*R*,3*S*,*Z*)-6-fluoro-*N*,*N*-bis(4-methoxybenzyl)-3-methyl-6-(4,4,5,5-tetramethyl-1,3,2-dioxaborolan-2-yl)hex-5-ene-2-sulfonamide (**A**)

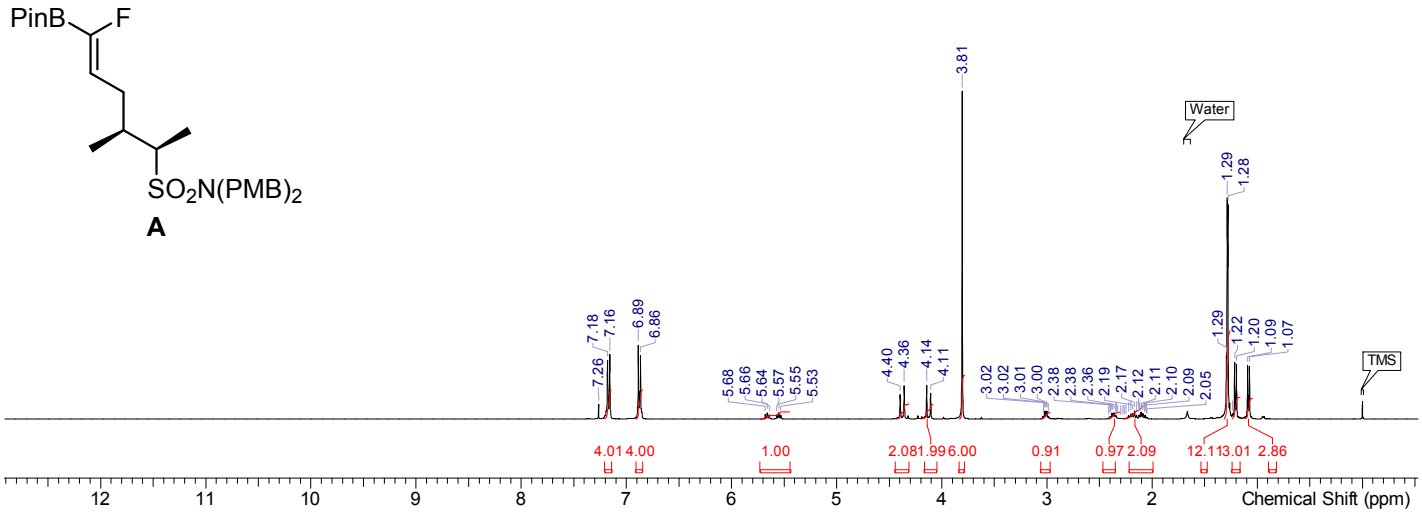

^{13}C {^{1}H} NMR (125 MHz, Chloroform-*d*) of (2*R*,3*S*,*Z*)-6-fluoro-*N*,*N*-bis(4-methoxybenzyl)-3-methyl-6-(4,4,5,5-tetramethyl-1,3,2-dioxaborolan-2-yl)hex-5-ene-2-sulfonamide (**A**)

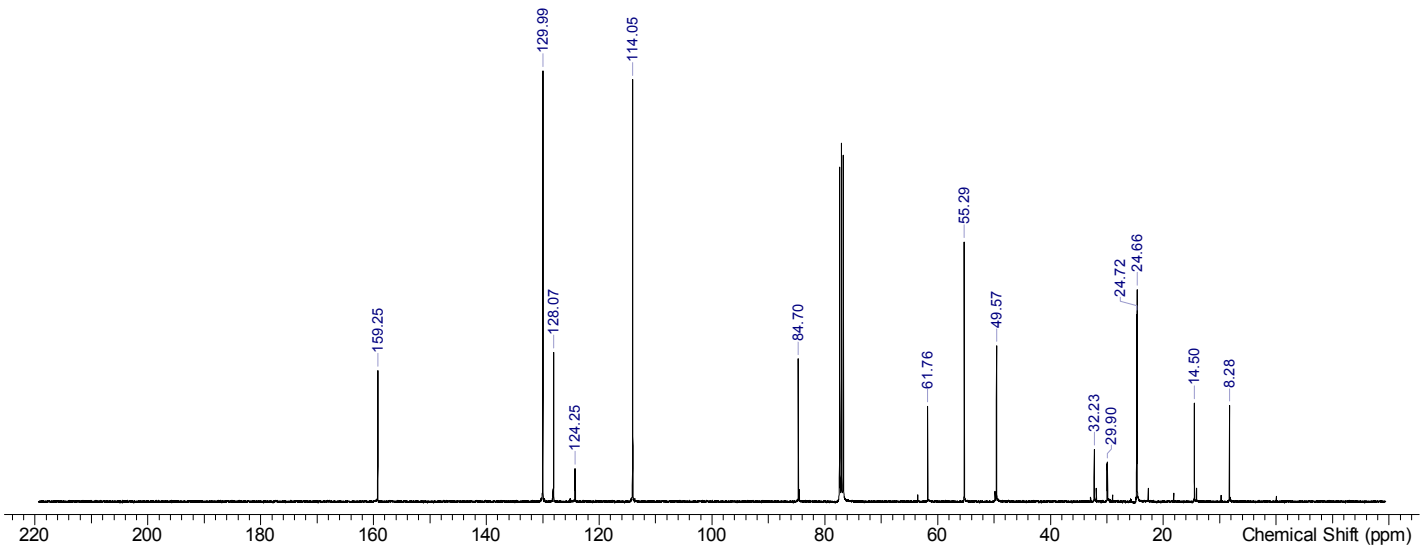

^{19}F {^{1}H} NMR (376 MHz, Chloroform-*d*) of (2*R*,3*S*,*Z*)-6-fluoro-*N*,*N*-bis(4-methoxybenzyl)-3-methyl-6-(4,4,5,5-tetramethyl-1,3,2-dioxaborolan-2-yl)hex-5-ene-2-sulfonamide (**A**)

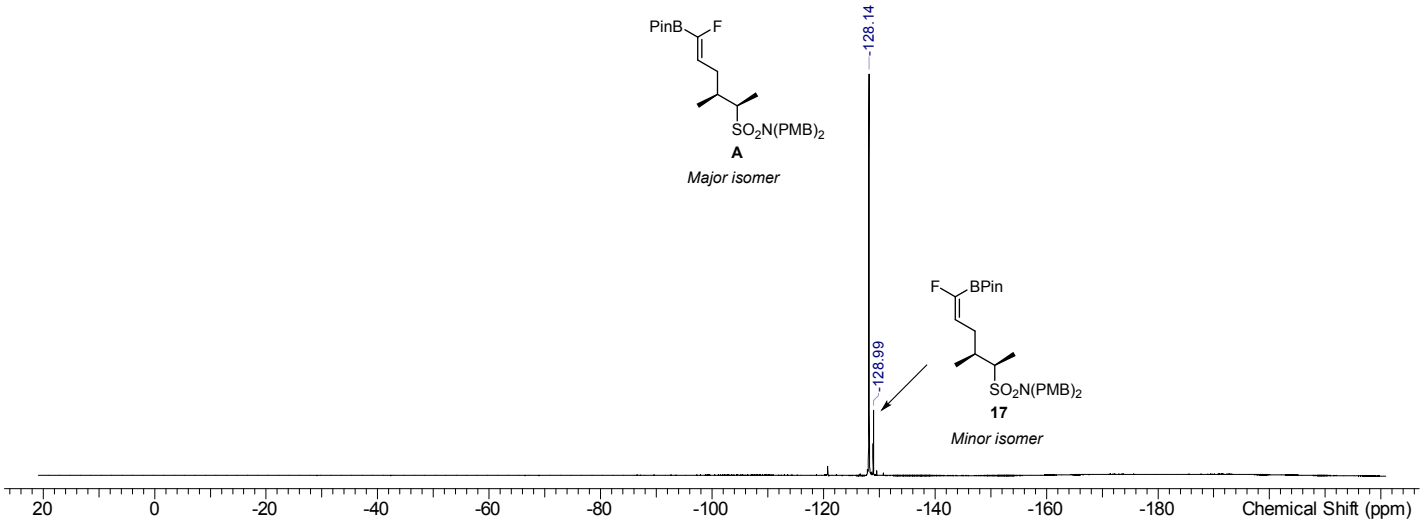

UPLC spectra of (2*R*,3*S*,*Z*)-6-fluoro-*N*,*N*-bis(4-methoxybenzyl)-3-methyl-6-(4,4,5,5-tetramethyl-1,3,2-dioxaborolan-2-yl)hex-5-ene-2-sulfonamide (**A**)

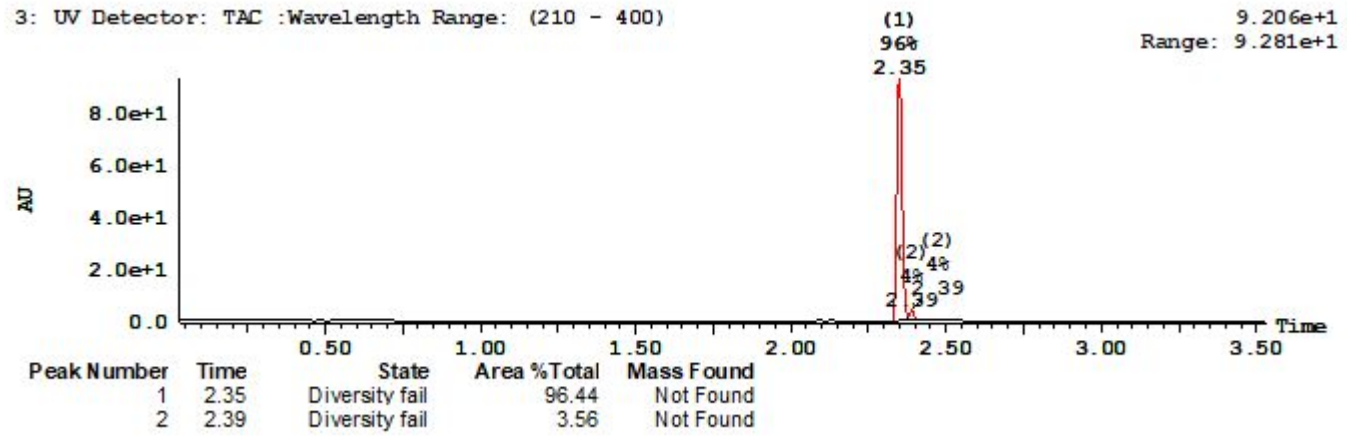

Peak Number	Time	State	Area %Total	Mass Found
1	2.35	Diversity fail	96.44	Not Found
2	2.39	Diversity fail	3.56	Not Found

2. Transient intermediates

^{1}H NMR (400 MHz, Chloroform-*d*) of 2-(((2*R*,3*S*)-6,6-difluoro-3-methylhex-5-en-2-yl)thio)pyrimidine (**13**)

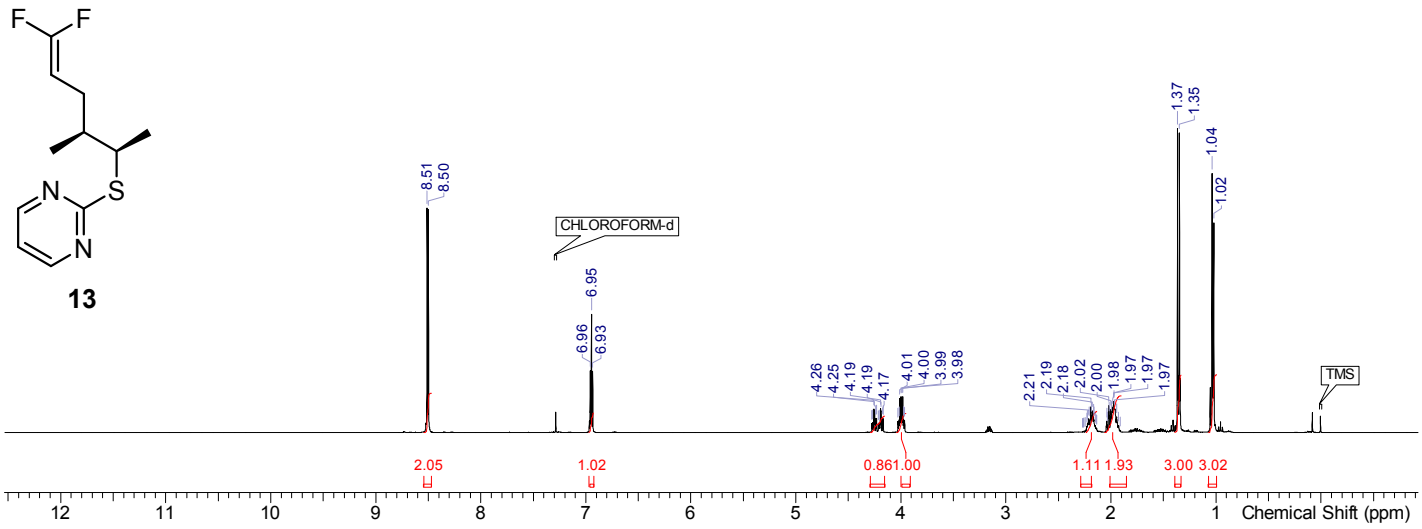

^{13}C {^{1}H} NMR (101 MHz, Chloroform-*d*) of 2-(((2*R*,3*S*)-6,6-difluoro-3-methylhex-5-en-2-yl)thio)pyrimidine (**13**)

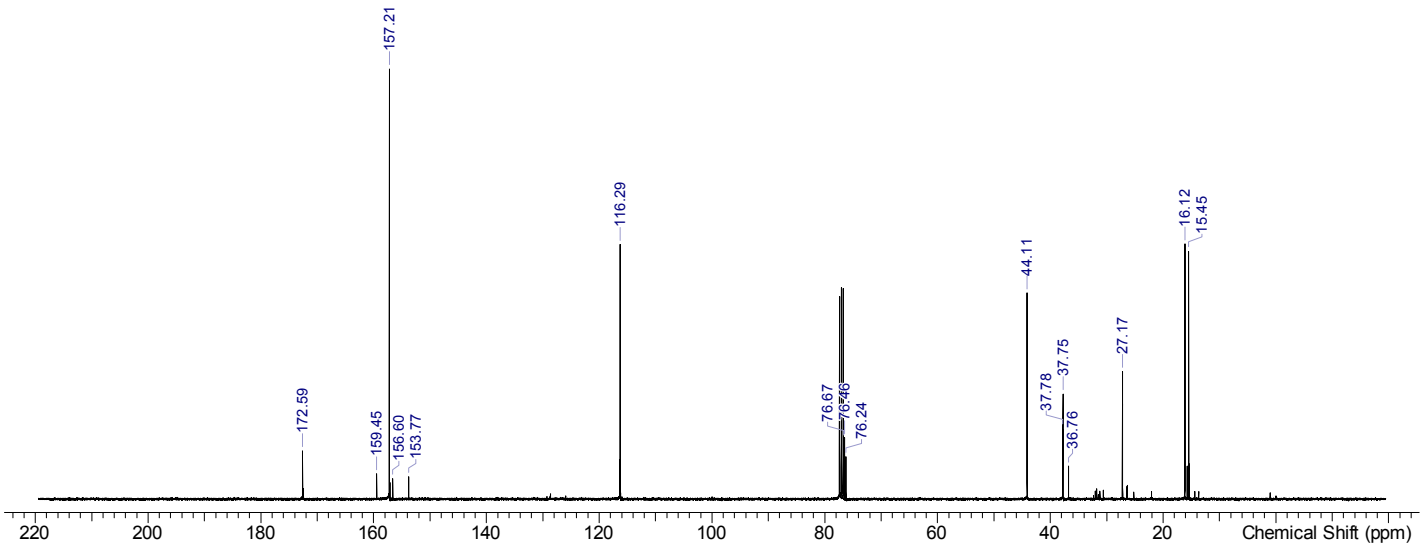

^{19}F {^{1}H} NMR (376 MHz, Chloroform-*d*) of 2-(((2*R*,3*S*)-6,6-difluoro-3-methylhex-5-en-2-yl)thio)pyrimidine (**13**)

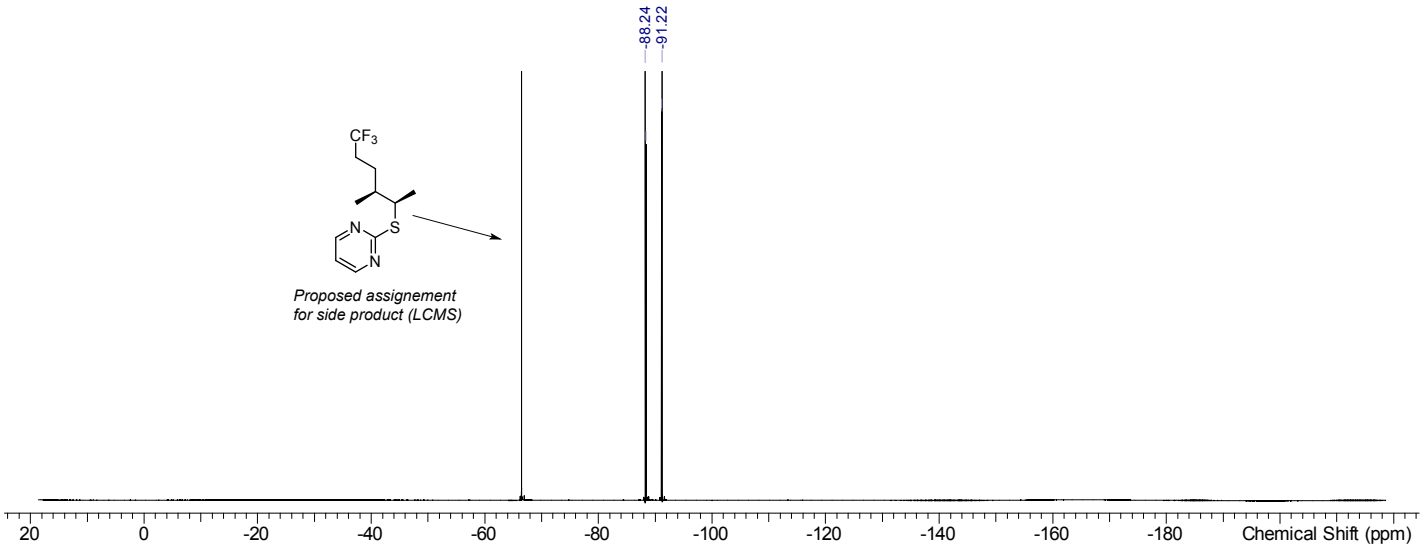

^{1}H NMR (300 MHz, Chloroform-*d*) of (2S,3S)-6,6,6-Trifluoro-3-methylhexan-2-ol (**9**).